Interner Bericht
DESY F41-76/08
September 1976

Synchrotron Radiation Sources:
Their Properties and Applications for VUV and X-Ray Spectroscopy

by

E. E. Koch

SYNCHROTRON RADIATION SOURCES: THEIR PROPERTIES AND APPLICATIONS FOR VUV AND X-RAY SPECTROSCOPY*

by

E.E. Koch
Deutsches Elektronen - Synchrotron DESY
Hamburg, Fed. Rep. Germany

ABSTRACT: Synchrotron radiation from accelerators and storage rings offers far reaching possibilities for many fields of basic and applied physics. The properties of synchrotron radiation, existing and planned synchrotron radiation facilities, as well as instrumental aspects are discussed. In order to illustrate the usefulness of the synchrotron radiation sources a few highlights from atomic, molecular, and solid state spectroscopy are presented and examples from x-ray experiments and from the field of applied physics are given.

* based on lectures at the Winter College on The Interaction of Radiation with Condensed Matter International Center for Theoretical Physics Miramare, Trieste 14 January - 26 March 1976.

To be published as Chap. 19 in "Interaction of radiation with condensed matter" L.A. Self, editor, publication of the Trieste Center for Theoretical Physics International Atomic Energy Agency , Wien 1976

1. Introduction

Although optical spectroscopy is now a well established science dating back to the early 19th century, the strong absorption of the atmospheric gases, Ozone at about 3050Å, Oxygen at 1850Å, and Nitrogen at about 1000Å, and the transmission cut off of quartz optical systems at about 1770Å had been for a long time the short wave length border line of the spectrum for most spectroscopists. Consequently in general only the outer valence electrons could be excited and their spectra studied in detail.

A few researchers such as Lyman and Schuman extended their experiments beyond this limit into the vacuum ultraviolet (VUV) [1]. Meanwhile the VUV (6 to 6000 eV corresponding to 2000 to 2Å has become an important part of the spectrum: the interaction of short wavelength VUV radiation with matter allows for an unrestricted investigation of the electronic structure of matter, including excitations from deep lying valence orbitals or bands and from inner shells and core levels, [2-4].

Most of the experimental studies were restricted however by the light sources available, generally the rare gas continua and a couple of fairly strong resonance lines. [5] In recent years, a major, probably the most important and real novelty for spectroscopic work in the VUV was the worldwide effort in the scientific use of synchrotron radiation (SR) as a source for spectroscopy and for structural analysis.

Synchrotron radiation is produced when a fast charged particle with an energy $>> m_o c^2$ is deflected in a strong magnetic field. Circular electron and positron accelerators and storage rings where the particles move with relativistic energies are the "natural" sources of this radiation, [6]. SR has a number of outstanding properties:

1. Intense continuum from the infrared out to the x-ray region.
2. High degree of collimation ($\sim$ 1mrad).
3. Polarization, completely linear in the plane of orbit.
4. Time structure, pulse duration as short as $\sim$100 psec.
5. Calculability of characteristics.
6. Clean environment (10^{-9} Torr), high stability of storage rings.

Thus, SR bridges the gap between the far UV and the x-ray range and the unique combination of the above characteristics offers far reaching possibilities for many fields of science and technology (Fig. 1).

The two most common techniques are absorption and reflection spectroscopy. Scattering, emitted fluorescence and electrons ejected by the radiation may also be studied. For the latter experiments, the possibility to study these processes as a function of the excitation energy, which can be selected from the continuum by various types of monocromators, is one of the major advantages. Furthermore, there are a number of experiments which very elegantly can make use of the white continuum of the radiation. The "history" and some of the major developments in the application of SR are sketched in Fig. 2.

It should be noted at this point that there does not exist a coherent field of research which one could name "Synchrotron radiation physics". The exploitation of the outstanding properties of this light source has now become an interdisciplinary effort where researchers from many fields of science ranging from atomic physics to chemistry, biology, and applied sciences come together. Consequently, the applications, which

we shall consider as illustrations for the potentialities of SR as a spectroscopic tool, can only be sketched by a few examples, mostly taken from the experimental programs in progress at DESY in Hamburg. For a detailed and more balanced discussion of the results we refer to a number of review articles [7-18] and to the fairly easy accessible original literature [19].

2. Basic Properties of Synchrotron Radiation

For a quantitative discussion of the properties of SR one generally starts with the analytical expressions for the total energy loss as well as the angular and spectral distribution for a monoenergetic relativistic electron on a circular orbit. These expressions have been derived by Iwanenko and Pomeranchuk [20] and in detail by Schwinger [21].

The total power radiated by such an electron is in c.g.s. units [21]

$$\int I\ (\lambda,\psi)\ d\lambda d\psi = \frac{2}{3}\ \frac{e^2 c}{R^2}\ \left(\frac{E}{m_o c^2}\right)^4 \qquad (2.1)$$

where R is the radius of the electron orbit, E its energy and where e, c, m_o have their usual meaning. One sees immediately why protons of identical energy would radiate far less power than electrons ($m_o c^2_{\text{proton}} = 1836.12\ m_o c^2_{\text{electron}}$) and how the total instantaneous power radiated by a single electron depends on the energy E and the orbital radius R.

In the above formula I as a function of the wavelength λ and the elevation angle ψ is given by [20,21]:

$$I(\lambda,\psi) = \frac{27}{32\ \pi^3}\ \frac{e^2 c}{R^3}\left(\frac{\lambda_c}{\lambda}\right)^4 \gamma^8 \left[1+(\gamma\psi)^2\right]^2 \left[K^2_{2/3}(\xi) + \frac{(\gamma\psi)^2}{1+(\gamma\psi)^2} K^3_{1/3}(\xi)\right] \qquad (2.2)$$

there, λ_c is the "cut off" wavelength given by

$$\lambda_c = \frac{4\pi R}{3}\ \gamma^{-3} \qquad (2.3)$$

and ξ is given by

$$\xi = \frac{\lambda_c}{2\lambda}\ \left[1 + (\gamma\psi)^2\right]^{3/2} \qquad (2.4)$$

where $\gamma = \sqrt{1-\left(\frac{v}{c}\right)^2}^{-1} = \frac{m_o c^2}{E}$ and $K_{1/3}$ and $K_{2/3}$ are modified, Bessel functions of the second kind [22].

The intensity decreases rapidly for $\lambda \leq \lambda_c$ whereas for $\lambda >> \lambda_c$ the intensity is almost independent from the energy E of the particle.

For practical applications other functions than $I(\lambda,\psi)$ such as $I(\varepsilon,\psi)$ where ε denotes the photon energy $\varepsilon = hc/\lambda$ might be more useful. Furthermore, it is often far more convenient to normalize the intensity to the circulating electron current j. For synchrotrons, where particles are accelerated from a minimum energy, with which they are injected, up to the final energy, one has to take into account the dependence of the particles energy on time during acceleration and usually an averaged power radiated off is calculated by taking one third of the current given as an effective current. Furthermore the finite size of the beam due to betatron and synchrotron oscillations about a mean stable orbit has to be

accounted for in considering real cases.

Thus for an easy comparison of the characteristics of various synchrotron radiation sources the following equations emerge:

$$N = 4.5\ .\ 10^{12} j\ \ R^{1/3}\ \varepsilon^{-2/3} \qquad (2.5)$$

which is valid for $\varepsilon << \varepsilon_c$, where N denotes the number of photons per sec per eV per mA in an infinitely high slice of one mrad horizontal width and where the current j is given in [mA], R in [m] and ε in [eV]. In this spectral range N is almost independent from the particles energy E. The cut off energy $\varepsilon_c = hc/\lambda_c$ is given by

$$\varepsilon_c = 2.22\ \ 10^3\ E^3\ R^{-1} \qquad (2.6)$$

For the storage ring DORIS in Hamburg as a specific example the intensity of SR radiated into a solid angle of 1 mrad x 1 mrad as a function of the photon energy is depicted in Fig. 3. The beam current j[mA] and the energy E of the circulating electrons are the parameters [23]. Note the high intensity over a very large spectral range.

The strong collimation of the radiation has already been mentioned. The radiation is emitted into a very small angular cone around the particles instantaneous direction of flight. Thus the plane of the accelerator is filled with radiation, while the emission in the off-plane direction is confined to a wedge of only about one mrad angular spread (Fig. 4). At the cut off energy ε_c the angular width $\langle\psi\rangle$ is $\langle\psi\rangle = 1/\gamma$. Further $\langle\psi\rangle$ varies roughly like $\langle\psi\rangle \propto (\varepsilon_c/\varepsilon)^{1/3}$ for $\varepsilon < \varepsilon_c$. The intensity of the radiation as a function of the elevation angle ψ against the orbital plane is shown for three photon energies at the top of Fig. 5 taking DORIS as an example [23,24].

The polarization characteristics of SR are also displayed in Fig. 5. The two factors in eq. 2.2 in square brackets are associated with the two components of the polarization. The first describes the component with the electric field vector $\underline{E}$ parallel to the orbital plane, the second where $\underline{E}$ is perpendicular to the plane. With

$$P = \frac{I_{\parallel} - I_{\perp}}{I_{\parallel} + I_{\perp}} \qquad (2.7)$$

as the definition for the degree of polarization one obtains for P as a function of λ and ψ

$$P(\lambda,\chi) = \frac{K^2_{2/3}(\xi) - \frac{(\gamma\psi)^2}{1+(\gamma\psi)^2} K^2_{1/3}(\xi)}{K^2_{2/3}(\xi) + \frac{(\lambda\psi)^2}{1+(\gamma\psi)^2} K^2_{1/3}(\xi)} \qquad (2.8)$$

Thus within the orbital plane (ψ=o) the light is completely linearly polarized (Fig. 5). The radiation out of the plane of the orbit is not an irregular superposition of parallel and perpendicular polarized components but elliptically polarized. It can be decomposed into left and right hand circularily polarized radiation as shown in the lower part of Fig. 5.

The time structure of the light pulses emitted from a synchrotron or storage ring is determined by the time structure of the orbiting particles.

The particles are accelerated and stored in bunches due to the fact that only a limited number of spatial intervals on the circumference of the accelerator can be filled with particles having a stable orbit. For example, at DORIS the number of bunches on the circumference is 480 while the length of each bunch is only 2-3cm corresponding to about 140 psec. Thus as far as the time structure is concerned SR from such a storage ring has outstanding properties: The radiation is emitted in short flashes of 140 psec. duration. For spectroscopic experiments the repetition frequency is a further important parameter. It is determined by the repetition frequency of the filled bunches. Maximum separation between two pulses is obtained in the "single bunch mode" when only one bunch of particles is on the orbit. In this case, the period of revolution determines the repetition frequency - in the case of DORIS, this is 1μ-sec. It should be noted that such a pulsed VUV - and x-ray SR source has a very high stability with nearly gaussian pulse shapes, constant amplitude and a quartz oscillator precision.

Synchrotron radiation is incoherent. In particular, the fields emitted from the same tangential point by two successive pulses are completely independent. As Benard and Rousseau [25] have shown the coherence length, defined as the maximum distance between correlated emission points is about $200 \cdot \lambda$, as long as the wavelength λ is smaller than the length of the electron bunch.

Finally, we mention as important properties of SR the fact that the above characteristics can be calculated with the aid of a small set of well defined parameters and that SR is generated in a clean ultrahigh vacuum (for storage rings) environment. These properties are very useful for practical applications e.g., calibration experiments or surface sensitive investigations.

3. Electron Synchrotrons and Storage Rings as Radiation Sources

An electron synchrotron accelerates electrons on a fixed circular orbit. Electrons are injected at a relatively low energy, say several 100 MeV from a linear accelerator. The synchrotron consists of an array of magnets for focusing and bending the beam and straight linear sections for accelerating the particles. The magnetic field in the deflecting magnets rises during the acceleration in order to keep the electrons on the same circular path when their energy is gradually increased. Note that the number of revolutions of one particle is roughly 10,000 in order to reach 1GeV energy. In the case of the storage ring, the magnetic field remains constant. The storage ring must be filled by an accelerator with electrons of the appropriate energy. Accelerator sections within the storage ring compensate for the losses due to synchrotron radiation. In Fig. 6, a schematic plan of the Deutsches Electronen Synchrotron (DESY) installation is given. The linear accelerator injects pulses of electrons or positrons into the synchrotron DESY. The particles can be accelerated up to 7.5 GeV. The synchrotron can also be used to fill the storage ring DORIS where the particles circulate in two beam pipes one above the other in opposite directions. They are allowed to collide at the two interaction regions. The four places where SR beam pipes are installed are also indicated.

3.1 Synchrotron Radiation Facilities

All the existing SR facilities at electron accelerators or storage rings are in three general classes: (i) symbiotic (with high energy physicists) use of operating high-energy physics facilities, such as the DESY installations described above, (ii) conversion of existing but no longer needed high-energy physics facilities to dedicated SR use, and (iii) construction and operation of dedicated facilities.

Ten years ago SR experiments were carried out only at a few places at the NBS (Washington) at INS (Tokyo) at Frascati (Italy) and at DESY (Hamburg). This situation has changed rapidly since that time as is obvious from Table I where the relevant parameters for accelerators and storage rings presently under consideration as SR sources are compiled. In this list the machines have been grouped according to their cut off energy ε_c into four major categories. Machines from group I and II are excellent sources for VUV and soft x-ray spectroscopy. With their low particle energies and small diameters, the restrictions imposed by radiation protection during operation of the machines are less severe and the access is more easy allowing for small distances between the source points and the instruments.

At larger machines (group III) also x-rays become available for spectroscopic purposes, at the same time making remotely controlled experiments and heavier shielding a necessity.

Interest in the use of even larger machines (group IV) for spectroscopic experiments has been only marginal. For the majority of experiments the hard x-ray component of these sources, which is difficult to eliminate, is only an unwanted by product. Furthermore the current in these machines is generally very low and the distance from the source point to the laboratory site is large because of the large radii.

3.2 Comparison with Conventional Sources

At this point it is useful to consider conventional light sources and compare them to SR sources. Recently Kunz [26] has collected the main points for such a comparison for the infared, visible, the VUV and x-ray range.

It seems as if the potential advantages of SR in the infared [27] have not been used for any application, probably due to the rapid progress in the development of tunable lasers for this region of the spectrum. In the visible part of the spectrum, ordinary sources and tunable lasers govern the field.

In the VUV below 2000 Å SR is superior to any conventional source because of the high intensity, polarization and tunability. This is schematically indicated in Fig. 7, where the dependence of the spectral distribution of SR on the energy of the particle is scetched and compared to the most commonly used rare gas continua [5,28,29]. The rare gas continua extend from the visible to beyond 600 Å with a maximum flux of 10^9 photons/sec Å (5×10^{10} photons/sec eV) at the helium maximum of about 800 Å. Similar values hold for the other rare gases (see Table II and Refs 5,28). Only the 21.2 eV HeI resonance line as emitted from a capillary discharge [30], has an intensity comparable to synchrotron radiation. The problem of gas contamination has, however, not been solved completely for the rare-gas lamps and both the emission

and absorption lines superimposed on the continua are severe limitations.

Below 100 Å down to 10 Å the intensity of classical x-ray tubes is weaker than that of SR. The BRV uranium rod source [31] with repetition rates of 1 to 2 shots per minute is in principle capable of considerable peak intensity.

In particular in the region below 10 Å an advantageous application of SR has to be discussed with the definite experimental goals in mind. X-ray tubes are characterized by an isotropic brightness (number of photons/ apparent area x unit solid angle x unit energy interval x unit time), whereas the high brightness of SR is restricted to a small vertical angle. Thus in all experiments requiring a high brightness in space versus total intensity, such as x-ray interferometry [32], x-ray topography [33] and x-ray diffraction [34] synchrotron radiation offers decisive advantages over x-ray tubes.

Quantitative values for the spectral distribution and the brightness of actual SR sources are shown in Figs. 3, 8, and 9. The horizontal angular segment of radiation which can be accommodated by an experiment depends on the distance of the experiment from the tangential point. This is an important fact when different SR-sources are compared to each other (see section 3 below). Where small distances are permissible and instruments are used which can accommodate more divergence of the SR beam a smaller accelerator can compensate for the difference in current compared to a more powerful machine. This is demonstrated in Fig. 8 where the intensity into a 2 cm x 2 cm wide window is given at laboratory distance d for different accelerators and storage rings.

The maximum brightness (photons/sterad x sec x cm^2 x eV) of the source which is obtained in the synchrotron plane, depends also on the size of the source. This is typically 2 mm high x 10 mm wide. Small storage rings at low current have beam heights as small as 0.1mm. This can be of considerable advantage. Comparison is made in Fig. 9 of SR with radiation from other sources [35,36] on the basis of brightness.

3.3 Dedicated Storage Rings

In Table I are listed already a number of storage rings which are exclusively planned or used for SR experiments. These machines offer a number of advantages over symbiotically used machines. The free choice of the particle energy E and the resulting cut-off energy ε_c, the choice of the pulse pattern and the control of beam size, shape, and position tailored to the needs of the SR-users are the most obvious advantages. Generally also a higher stability can be achieved. Finally, the inclusion of special features and options into a dedicated machine is much easier. As such special features wavelength shifters or wigglers (see below), build-in optical devices e.g., integrated monochromators which collect very wide horizontal apertures or beam deflectors may be considered. With the help of the latter the beam position may be changed periodically in order to achieve wavelength modulation in combination with especially designed monochromators.

These considerations and the growing needs of the spectroscopists have lead to further recent design studies for dedicated SR facilities at a number of places. Two basic concepts emerge: (i) a storage ring of $\sim$ 0.7 to 1 GeV, attractive for most VUV and soft-x-ray applications

(i.e. $10 \leq \hbar\omega \leq 10^3$ eV). Such a machine could in addition to experiments in basic research also be used in industrial applications for duplications of device masks by soft-x-ray lithography (see Section 2). As an example, we mention the state-of-the-art design study for the storage ring "Adaddin" of the Stoughton Synchrotron Radiation Center [38] (energy $\sim$0.75 GeV, radius $\sim$2 m, proposed current 500 ma and a cut off energy $\varepsilon_c \sim$ 450 eV). (ii) a high energy storage ring ($\geq$ 2 GeV) for x-ray applications ($\hbar\omega \geq 10^3$ eV). As an example the 2 Gev synchrotron radiation source NINA II at Daresbury [39] may be quoted (energy 2 GeV, radius 5.56 m, current 1000 mA and ε_c = 3200 eV). Such a ring can, of course, also provide radiation for $\hbar\omega_c \geq 10^3$ eV and possibly offers greater brightness than a lower energy ring. It also seems possible to use a smaller ring (i) as part of a facility having a higher energy storage ring for x-ray applications. Thus the smaller ring would serve both as an injector for the larger ring and as a convenient primary source for $\hbar\omega \leq 10^3$ eV.

The costs for a storage ring with $\varepsilon_c \geq$ 3KeV start to rise rapidly as critical energies above 3KeV are demanded. Thus, in spite of the inconvenience of symbiotic use of a machine with a high energy physics program, use of SR in the far x-ray region from existing high energy machines still seems to be appropriate.

3.4 Wavelength Shifters, Wigglers, New Developments

With the steadily increasing technological skills in accelerator design and the growing experience in operating such machines very interesting devices for extending the capabilities of SR-sources have become feasible. The principle of the two most frequently discussed devices, the wavelength shifter and the wiggler, is sketched in Fig. 10.

The wavelength shifter seems particularly useful for extending the spectral range of smaller machines. Introduction of suitable bending magnets into the storage ring magnet-lattice results in a local reduction of the radius and hence according to eq. 2.3 in an extension of the spectral distribution to smaller wavelength [40].

An introduction of multipole wiggler magnets, that is, a series of periodic bends into the path of a relativistic electron beam by a periodic transverse magnetic field, could yield radiation which is to a certain extent coherent [41]. The local magnetic field can be made much larger than the ring magnetic field. The collimation of the SR remains, since ε_c is increased by a factor n, where n is the number of wiggles put in series.

Recently Kincaid [42] proposed to use a helical magnetic field in order to make the electrons move in short period helical orbits. According to his calculations such a device would yield quasi monochromatic light with a band width that depends on the number of periods in the helical magnet, the energy resolution of the electron beam and its angular divergence.

Possibly the most exciting perspective is the possibility to build a free-electron laser completely tunable from the infrared through the VUV region. Recent experiments performed by a group at Stanford University [43] show that a free-electron laser, one in which free electrons stimulate the emission of magnetic bremsstrahlung in a spatially periodic transverse

magnetic field [44,45], could be a practical device.

In concluding this section, we mention as a related phenomenon the possibility to use Compton Scattering of photons from relativistic electrons for the generation of polarized high energy x-rays [46,47]. As Yen [48] has pointed out presently available technology, namely intense lasers as the photon source and electron storage rings with high currents and good stability, seems adequate to construct an intense, and polarized γ-ray source.

4. Some Instrumental Aspects

It follows from the discussion of Sections 2 and 3 that electron accelerators and storage rings are in principle unique light sources in the VUV and x-ray region. In order to make profitable use of these machines one has to consider however a number of other aspects like access, choice of specific monochromators and particular experimental arrangements as indicated by the sequence of boxes in Fig. 11.

Beam Access

For an easy access to the SR sources and in order to have working conditions similar to those in conventional laboratories several instrumental developments were necessary. There are the more trivial points like safety requirements making remotely controlled experiments a necessity in many cases and the vacuum requirements imposed on the experiments by such a clean source. In a number of facilities several radiation beam lines were installed making simultaneous experiments on more than one instrument possible. Where the installation of additional beam lines was not feasible splitting of the beams by one or more grazing incidence mirrors provided several independent beams at laboratory site. The beam line system and the arrangement of the various experiments in the SR-laboratory at the DORIS storage ring [23], as schematically shown in Fig. 12, serves as an example.

Monochromators

The SR light sources are fixed and impose some restrictions on the design of monochromators. This is why in addition to conventional mountings (eventually slightly modified) a number of new instruments have been developed especially adapted to the source geometry and characteristics of synchrotron light. The continuous spectrum is monochromatized by normal incidence (visible to 45 eV range) and grazing incidence (20 to 500 eV range) grating instruments. Due to the polarization properties and source geometry vertical reflection and dispersion planes and horizontal slits are preferred. We note that no useful instrument for the range from about 500 eV to 1.5 KeV has been described yet.

In the normal incidence range (visible to 45 eV) conventional types of monochromators like the McPherson normal incidence type or Seya mountings have been utilized. For a general description of these instruments, see e.g., Ref. 5. A modified Wadsworth mounting very suitable for the source geometry of a synchrotron or storage ring has been developed by Skibowski and Steinmann [49]. The instrument operates without an entrance slit and achieves with only one single optical component, namely the grating rotating around an excentric pivot, a medium resolution of i about 2Å and a high flux at the exit slit. With a vertical mounting of such an instrument [50], an even better resolution of 0.5 to 1 Å was

obtained. Recently, Saile et al. [51] have described a new experimental set up with a 3m normal incidence monochromator for photon energies from 4 to 45 eV. With this instrument, having a vertical dispersion plane (see Fig. 13), high resolution spectroscopy becomes possible in the VUV with rapid photoelectrical scanning of the spectra and a resolution of 0.03Å in first order.

The grazing incidence region presents more difficult problems, e.g., superposition of higher orders and more complicated imaging than the normal incidence range. This has lead to the development of several new instruments in addition to the classical Rowland mounting, Kunz [52] has reviewed the specific problems encountered in this spectral region and discussed a number of instruments. A comprehensive survey on grazing incidence monochromators designed for use with synchrotron radiation [53-57] is given in Table III. All of these instruments have to compromise in one way or the other on the requirements of high efficiency, high resolution, good order-sorting capability and simplicity in design (e.g., fixed exit beam for attachment of massive experimental set ups). Since not all of these requirements are achievable in one instrument the actual choice of a particular mounting depends on the needs of the planned experiment.

As an example a semischematic layout of the grazing incidence monochromator as described by Dietrich and Kunz [58] is shown in Fig. 14. This instrument operates with a plane premirror, a plane grating and a focusing mirror, with all three elements moving in a coupled motion. In this way, a fixed position of the exit slit and a fixed direction of the exit beam is achieved. By a careful choice of the parameters of the instrument virtually no higher order admimixture occurs over the whole wavelength range from 40 - 350Å. Using the same optical principle Eberhardt et al. [59] have built an UHV-version of this instrument "Flipper" where the sliding premirror of the original instrument is approximated by six different pre-mirrors each of them with two different surfaces for optimizing suppression of higher orders.

For the range below 10 Å, where crystal monochromators have to be used, the techniques how to monochromatize SR and to eliminate harmonics in the most appropriate way, have been described recently by Bonse et al. [60] and Beaumont and Hart [61] have discussed a multiple reflection version of the classical crystal diffractometer for SR - x-ray applications. The remotely controlled optical bench incorporating two focusing premirrors and a bent quartz crystal monochromator as described by Barrington Leigh and Rosenbaum [62], is schematically shown in Fig. 15.

As examples for further very interesting new instrumental developments, we mention here the interferometer for SR-x-ray interferometry as developed by Bonse and Materlik [32,63], the use of zone plates for imaging in an x-ray microscope by Niemann et al. [64] (see Section 5), the time of flight electron spectrometer as developed by Bachrach et al. [65] making use of the time structure of the SR source and a number of modulation experiments [66,67,68].

Finally, data handling should be mentioned, when experimental aspects are discussed. An advanced interactive system for the evaluation of spectroscopic data has been set up at DESY for SR users [69]. It is capable to perform data acquisition, processing, and reduction of the input data, and more complicated data handling such as a Kramers-Kronig

analysis. A further system directly linked to the experiments is available at the DORIS SR-laboratory.

5. Examples of Experimental Results

In the following only a very small selection from the large number of experimental results obtained with SR can be given. A number of topical review articles are available for the use of SR in atomic [11,13,20] molecular [11,13,16] and solid state physics [11-18,71] reflecting the broad spectrum of activities. Interest in the x-ray part of the spectrum is of more recent vintage. For a synopsis of the various experiments and some references to the original literature, see Fig. 1 and Tables IV, V, and VI.

5.1 Atoms and Molecules

The fine structure near the onset of the absorption of a particular shell as well as the absorption cross section in the range of transitions into continuum states far above onset has been investigated for a series of atoms and molecules with the use of SR. Spectra as shown in Fig. 16 for krypton [93] provide a large amount of detailed information as regards the electronic structure of the free atom and excitations from various subshells. In particular, in almost all cases, "sawtooth" like absorption at the onset of a new shell as familiar from x-ray spectra is missing and a delayed onset due to a potential barrier or strong resonance lines are observed instead. Comparison of the gaseous and solid phase e.g., in the range of the 3d transitions in Kr (Fig. 16) reveals the local character of the states involved in the spectrum form the solid. Spectra in the VUV are now available for all rare gases [17] for a number of metal vapours [73-77] for alkali-[73] and for alkaline earth-atoms [74]. In Fig. 17 are shown the spectra from metallic and atomic barium in the range of the 4d shell excitations [75]. These spectra, also obtained at other laboratories [76,77] have been discussed in detail by Wendin [94] in his theoretical investigation of many body effects. They constitute the proving ground for theories of the collective response of electron shells in the process of photoionization, as advanced by Amusia and collaborators [95]. For instance, the broad maximum in the cross section at about 110 eV in both phases of Ba has been ascribed by Wendin [94] on the basis of his calculations as caused by a strong collective resonance of the electrons from the 4d subshell.

As an example for the resonance-like structure in inner shell spectra the analysis of the 4d → np type transitions in Xe above 64eV as discussed in detail by Ederer and Manalis [96] is shown in Fig. 18. An important point is that here only transitions into np-type final states are observed and that the d→f transitions cause a large maximum in the continuum delayed towards higher energies. This has been explained as a centrifugal barrier effect by Cooper [97].

Recent studies of the valence shell excitations of the rare gases Xe, Kr and Ar under high resolution ($\Delta\lambda = 0.03$Å) in the range of autoionization revealed Rydberg states with main quantum numbers n, up to $n \geq 40$ superimposed on the first continuum (Beutler - Fano- resonances) [98] (see Fig. 19). Anomalies in the s and d series due to interference effects could also be observed. The high resolution at low gas pressure made the investigation of field quenching of the highly excited

Rydberg states in weak static electric fields possible.

As an example for the detailed information obtainable from photoelectron spectroscopy of atomic gases, we mention the experiments of Houlgate et al. [82] in which the β parameters could be determined over a fairly large energy range. Their results for the Ar 3p electrons, when compared to theoretical predictions enabled an unambiguous decision to be made in favour of the theory of Amusia (RPA) [95] against the Hartree-Fock calculations of Kennedy and Manson [99]. Turning now to molecular spectroscopy we leave out the many absorption measurements on atmospheric [78,79] and simple inorganic molecules, e.g., [80,81] which provided a vast amount of new information. Spectra for the valence shell absorption of a number of simple organic molecules such as alkanes [50], benzene [100] napthalene and anthracene [101] have been measured and compared to existing theoretical predictions of excited molecular states. The comparison of gaseous and solid phase yields interesting information also in this case. If single crystals of these materials are studied [92] they may be considered in a first approximation as an oriented gas and the response of such crystals to photons is highly anisotropic. Consequently, the high degree of polarization of the SR is of considerable help in such experiments [16].

The fine structure at the carbon 1s K-edge in the range $280 \leq \hbar\omega \leq 300$ eV has been measured recently [102] for a number of simple hydrocarbons. The spectra being fairly simple compared to the valence shell absorption are characterized by weak maxima for energies below the ionization threshold for C 1s in the case of methane and ethane, whereas additional strong resonances are observed in the spectra from molecules containing π-electrons (see Fig. 20). These highly excited states have been assigned as either 1s → Rydberg or 1s →π* excitations on the basis of their term values and oscillator strengths.

In a series of papers Baumgärtel and coworkers [88] have discussed the photoreactions of small organic molecules studied by absorption-, photoion-mass- , and resonance photoelectron spectroscopy. As an example the resonance photoelectron spectra of halogenated methanes are shown in Fig. 21. These spectra were recorded by collecting zero or nearly zero energy electrons while varying the energy of the incident photon beam. Advantages of this threshold photoelectron spectroscopy [103] making very efficient use of the SR-continuum are the constant transmission of the electron analyzer, the accurate energy scale given by the wavelength setting of the monochromator and the suppression of angular distribution effects of the electrons. By investigating the fragmentation processes for the molecules shown in Fig. 21 it could be shown that the stability of the parent ions decreases with increasing symmetry of the parent molecules [88].

The continuum of SR makes possible also another mode of photoelectron spectroscopy where the energy distribution of photoelectrons is measured for various fixed excitation frequencies of the exciting light. By measuring the relative intensity of each group of electrons originating from different orbitals as a function of the excitation energy the branching ratios and the partial photoionization cross sections can be determined. Such experiments are in progress for a number of molecules [83]. They are also important for the interpretation of photoelectron measurements of molecules adsorbed on surfaces [104].

Another area of current experiments with SR is the investigation of the decay of excited molecular states via fluorescence or fragmentation. As an example, we mention the dissociative decay of NO studied by Hertz et al. [105]. In Fig. 22, the relative yields of NO^+, O^+, and N^+ as a function of the exciting wavelength between 550 and 650 Å are shown. It turns out that higher (neutral) Rydberg states of the molecule strongly influence the decay channels giving rise to the marked structure observed in the yield spectra. Similar experiments have been reported in a number of papers by Lee et al. [85].

An interesting and unique application of SR for molecular spectroscopy are the fluorescence decay experiments with a very good resolution in time by Lopez - Delgado et al. [86] in which use is made of the pulsed structure of the SR source.

5.2 Solids

Up to now, SR found its most fruitful application in the investigation of the electronic structure of solids. The various investigations (see Table V) centered around a better understanding of the band structure, of quasi particles such as excitons, which as in the case of rare gas solids govern large portions of the spectra (see e.g., Fig. 16), the elucidation of edge anomalies manifested as increased absorption spikes at the onset of the absorption from inner shells in metals, surface - and many body effects. As extensions of absorption and reflection spectroscopy sensitive experimental techniques such as thermomodulation or electroreflectance have been developed for use in the VUV and also the preparation and characterization of samples has improved considerably. As secondary processes optical-[18,87] and photoelectron emission [18,71] have been studied for a variety of materials. Tunability of the exciting light offers in such experiments the possibility to selectively excite a particular state, to separate the contributions from initial and final states to the photoelectron energy distribution spectra and to enhance or lower the probing depth of the measurement by exploiting the energy dependence of the electron attenuation length in solids [71]. New convenient modes of photoelectron spectroscopy could be developed by the use of SR. For instance for the constant initial state spectroscopy the electron analyzer pass energy is scanned simultaneously with and at the same rate as the exciting photon energy. [121] For all these developments we can again give only a very small selection of illustrative examples.

Much information on the band structure of solids has been inferred from optical data obtained by absorption and reflectivity measurements. In the upper part of Fig. 23 the absorption spectra of single crystalline and amorphous GaP in the energy range from 16 eV to 30 eV [122] are presented as an example. The maxima in the spectrum from the single crystal are due to spin orbit split transitions from the Ga 3d levels. The D_{III}^1 and D_{III}^2 double structure corresponds essentially to transitions to the two lowest conduction bands [122]. In the lower part of Fig. 23, the electroreflectance spectrum of crystalline GaP in the same energy range [68] is shown. The amount of additional information available from the modulation spectrum enhancing weak structures is obvious. The detailed assignment of such spectra and their correlation to the band structure is, however, not an easy task [18,68].

Photoelectron energy distribution measurements using SR have contributed significantly to a detailed understanding of the band-structure [71,106]. In Fig. 24, the photoelectron energy distribution curves for solid Ne, Ar, Kr, and Xe [123] are shown. These data demonstrated that almost all available band structure calculations for rare gas solids, often considered to be the most simple solids, fail to predict quantitatively other features than the spin orbit splitting.

As an example for the determination of partial emission intensities of various initial states to the photoelectron energy distribution spectrum we refer to an experiment by Eastman and Freeouf [124]. Several photoelectron energy distribution curves for NiO (100) are shown in Fig. 25. Contributions from different states can be disentangled by observing their characteristically different $\hbar\omega$ - dependent photoelectric cross sections. The emission due to localized 3d states and oxygen derived valence 2p bands are shown by the dashed and broken lines respectively. The d-state features are almost independent of $\hbar\omega$ whereas the p-band emission is gradually decreasing with increasing photon energy. In the XPS spectrum the p-band has almost disappeared and cannot really be observed.

Angle resolved photoemission measurements can give significant additional information. As an example, the polar diagram of the photoemission intensity for a KCl single crystal is presented in Fig. 26 as obtained by Himpsel and Steinmann [125]. Most remarkably, below the electron-electron scattering threshold the pattern depends only on the final energy irrespective whether the level has been populated by excitation from the valence band of the K^+ 3p core level. This can be taken as an indication for the fact, that due to electron-phonon scattering the electrons leaving the sample have lost the information about their initial states.

Optical, as well as photoemission experiments, have also successfully been used to study surface effects, that is, the occurrence of surface excitons [116], unoccupied surface states [115] and electronic states of adsorbates [104].

In order to illustrate the current debate about edge anomalies in simple metals, the Li 1s [126] and Na 2p [127] absorption edges are depicted in Fig. 27. From the different explanations proposed the many electron theory of the threshold anomaly by Mahan [128] Nozires and deDominicis [129] was the most attractive one because it could account for both the rounded edge in Li and the spike at the Na edge. It obtained support for the case of Na by the observation of an enhancement at threshold in both the solid and the liquid phase [118]. For Li, however, recent measurements of the partial photoyield from massive specimens taken at 77K showed that the Li K-edge is really composed of two parts [119]. The new results are in good agreement with the predictions of the one electron theory [130], taking Auger and phonon broadening into account.

5.3 X-Ray Experiments

Interest in using the x-ray part of the SR-spectrum has increased considerably during the last several years. Table VI gives a list of experiments performed or proposed and some representative references to the original literature, where more details can be found. In the following we will mention only a few of these experiments.

X-ray absorption edges and the structure found above the edges have been studied both experimentally and theoretically for some time [133]. The current view of the origin of the extended x-ray absorption fine structure (EXAFS) found above about 100 eV from the edge, is that the normal atomic absorption matrix element is modulated by the interference of outgoing photoelectrons with those backscattered from the nearest neighbours. Consequently, one seeks to obtain structural information, i.e., accurate interatomic distance information, from an analysis of the observed EXAFS structure e.g., [131,132]. For these high resolution K-edge-absorption studies SR from a storage ring offers intensity improvement over a powerful conventional source by a factor of 5×10^4 [131]. Thus, EXAFS measurements within half an hour with an excellent signal to noise ratio become possible. At SPEAR EXAFS-studies for structural investigations on a variety of compounds have now been completed or are in progress including such materials as organometallic molecules, which are of biological interest.

Presently it seems as if the theories used to date to analyze EXAFS data are still not sufficient in order to obtain quantitative agreement with experimental data. Nevertheless, atomic-shell spacings around an absorbing atom have been determined by empirically adjusting parameters and trying to fit the experimental curves [132].

Energy Dispersive X-ray Scattering [144], made possible by the development of energy discriminating x-ray detectors with high accuracy and resolving power, makes excellent use of the characteristics of SR. The method until recently exclusively carried out with Bremsstrahlung from conventional x-ray tubes, is illustrated in Fig. 28. A parallel beam of polychromatic SR x-rays falls on a sample. For a selected scattering angle Θ there will appear a number of wavelength which fulfill the Bragg condition. Recently, Bordas et al. [136] using the NINA Synchrotron and Buras et al. [137] working at DESY reported some preliminary results. In Fig. 29 the energy dispersive spectrum of iron powder as obtained by Buras et al. [137] is shown as an example. It is clear already from these first tests that SR due to the high brightness of the source and the resulting short exposure times together with the special features of the energy dispersive method (e.g., simultaneous appearance of all reflections and a fixed scattering angle) is very suitable for structure studies. Investigations of phase transitions and of time dependent phenomena where the pulsed structure of the SR-source may be used seem also possible and very promising.

The value of SR for x-ray topography has been first explored by Tuomi et al. [33,138] and later in some more detail by Hart [139]. For topography, the high intensity and in particular, the collimination of SR proved to be most advantageous. With these experiments, it could be shown that transmission and diffraction topographs taken with SR can have the same resolution as the best taken with laboratory sources. As an additional advantage larger areas could be covered with one exposure in times of a few seconds and many different topographs could be obtained simultaneously. For an example, see Fig. 30. Recently, Bordas et al. [140] have used SR in order to study phase transitions at the ferroelectric-paralectric phase transition in barium titanate with x-ray

topography. It is anticipated that in the future high speed topography using SR with X-ray sensitive vidicons or with conventional television and phosphor screens with exposure times below 1 sec. will become feasible.

Obviously, the extension of microscopy down to smaller dimensions with the help of x-rays would have many useful applications. To build an x-ray microscope is, however, not feasible with normal refractive optics, since the refractive index of all materials in the soft x-ray region is only slightly less than unity. Thus other means have to be employed to operate an x-ray microscope with SR.

In a simple design, Horowitz and Howell [141] have used an x-ray condensing mirror under grazing incidence to focus SR onto a collimating 2 µm pinhole. By illuminating a sample with the resulting pencil like polychromatic x-ray beam in a raster pattern and monitoring the characteristic fluorescent x-rays they obtained element disciminating pictures of specimens up to 100 µm thick in an atmospheric environment. No attempt was made, however, to form a focused x-ray image and consequently the resolution was roughly the same as the diameter of the collimated x-ray beam ($\sim$ 2 µm). An alternative approach without focusing was taken by Spiller et al. [142] using soft x-rays from a synchrotron for micrography. Already in a first test experiment a resolution below 1000 A was obtained (see below).

Niemann, Rudolph and Schmahl [64] were the first to employ real imaging of SR - x-rays with the help of a zone plate diffraction optical system (Fig. 31). Diffraction optics for x-rays have become possible by using holographically produced zone plates [145] with large zone numbers [146]. In this zone plate microscope, SR is dispersed by a holographic grating. A holographic zone plate (5mm diameter, 2400 zones) focuses one particular wavelength at a point in the object plane. The object is then imaged by a holographic micro-zone-plate with a ratio of 1:15 onto a photographic film. With a prototype set up a resolution of approximately 0.5 µm was obtained. This resolution can be increased considerably. In Fig. 32 an example of a wire mask as a test object is given. It should be noted that in this case monochromatic light was used, thus microscopy with variable x-ray energies in order to selectively enhance the contrast for a given element is possible.

The effort by Aoki, Ichikara and Kikuta who obtained an x-ray hologram by using SR [147] is also worth mentioning in this context.

X-Ray Micrography and X-Ray Lithography The combination of intense SR as a soft x-ray source, an x-ray resist as detector with high resolving power and a scanning electron microscope for viewing the resist profile has been used by Spiller et al. [142] as a powerful technique for the study of biological objects. The principle of this technique is illustrated in Fig. 33. The specimen is brought into contact with the x-ray resist supported by a wafer. It is illuminated with a parallel x-ray beam. After exposure and development of the resist a relief like replica of the absorption pattern of the object remains, which when coated with a thin metal film, is ready for viewing in a scanning electron microscope. Examples of the resulting micrographs of biological objects obtained with SR radiation from DESY, reflected from a gold mirror with 4° glancing angle are shown in Fig. 34. During these experiments, DESY operated at 3.5 GeV and 8 mA and the exposure times ranged from 4 to 10

minutes. These parameters can even be improved when working with a storage ring. The first experiments already demonstrated the great potentialities of this technique: The natural high degree of collimation of SR minimizes losses in resolution by penumbral blurring and a resolution close to 100 Å seems to be possible. The high intensity of soft x-rays available from a SR source drastically reduces the exposure times which might even be pushed below one second.

The technical application of this procedure for x-ray lithography is evident. In this case, the "specimen" is a device mask generated by a scanning electron beam system. Exact, fast, and cheap replications of such masks with patterns as small as 100 Å linewidth seem possible with the present day technology. Actually, Spiller and coworkers [143] have in the same run of experiments, successfully used SR for the replication of bubble memory patterns and zone plates. By using only the soft component of the spectrum masks with very thin absorber patterns could be copied with linewidth down to 500 Å. The control of other parameters important for practical applications such as heating of the wafers exposed to SR resulting in loss of resolution and radiation damage in the masks proved to be no problem. The authors conclude [143] that a dedicated storage ring would be a very desirable light source for x-ray lithography, for many applications far superior to a conventional source due to its collimation and intensity.

5.4 Applied Physics with Synchrotron Radiation

The advances in basic research in the VUV mentioned above suggest that within the next decade in addition to basic science also a VUV-technology oriented towards applied problems will be developed.

For instance SR holds great promises as an important technique in molecular biology as has been discussed recently by Holmes [148]. Some other areas like x-ray microscopy, x-ray lithography, time resolved topography and EXAFS for structural analysis have already been mentioned. There are a couple of other aspects of the application of SR which we would like to mention here briefly.

The accurate knowledge of absorption cross sections and dielectric constants for all kinds of materials in the gaseous and solid phase throughout the VUV might find useful applications, e.g., in plasma physics, atmospheric physics, and laser technology. The vast amount of data now available for these purposes has been collected and critically reviewed only for a small number of materials [e.g., 149]. Further data compilations, although in themselves scientifically not very exciting goals, might turn out to be very useful for many applications.

Experiments on optical multilayer coatings by which the normal incidence reflectance can be raised by almost a factor of 10 at around $\lambda = 190$ Å [150] promise progress in the design of high quality imaging elements (mirror microscopes and telescopes) for soft x-rays.

At several SR-laboratories, calibration experiments are in progress, e.g., Ref. [151,152]. In these experiments use is made of the calculability and high stability of SR from storage rings. As a further application we mention also that the pulse shape of SR from ACO has been used to study the time resolution of high speed photomultipliers with bialkali cathodes and its dependence on the incident photon energy [153].

6. Conclusion

Experiments with SR have matured in many ways from the use of an unwanted byproduct of high energy electron accelerators to a systematic effort to make VUV-radiation available to scientists from basic and applied physics research groups, to chemists and to biologists. It was the aim of these lectures to outline the present status of the field. It should be apparent that SR as a tool for research has an assured future for some time to come.

Acknowledgement

In the preparation of this paper, I have received help from many colleagues in the form of Figures and preprints. Special thanks go to C. Kunz and V. Saile for their comments and suggestions and a critical reading of the manuscript. It is a pleasure to acknowledge the hospitality of D. Eastman and his group at IBM Yorktown Heights during the period when this manuscript was completed.

Table I Synchrotrons (SY) or storage rings (ST) used (or considered) as light sources. E, particle energy; R, magnet radius; I, max current (during acceleration for SY); ε_c, critical photon energy

Name and location	Type	E(GeV)	R(m)	I(mA)	ε_c(eV)	Remarks
Group I, ε_c = 1 - 60 eV						
Tantalus I (Stoughton)	ST	.24	.64	100	48	dedicated
Surf II (Washington)	ST	.24	.83	∿30	50	dedicated
INS-SOR II (Tokyo)	ST	.3	1.1	∿50	54	dedicated
Group II, ε_c = 60 - 2000 eV						
Bonn I (Bonn)	SY	.5	1.7	30	163	SR Lab
ACO (Orsay)	ST	.55	1.11	35	333	dedicated
C-60 (Moscow)	SY	.68	2	10	349	
Frascati (Frascati)	SY	1.1	3.6	15	821	
PACHRA (Moscow)	ST	1.3	4	∿100	1220	dedicated SR Lab
Adone (Frascati)	ST	1.5	5.0	60	1500	SR Lab
Sirius (Tomsk)	SY	1.5	4.23	20	1770	SR Lab
Group III, ε_c = 2 - 30 keV						
Tantalus II (Stoughton)	ST	1.76	4.5	100	2690	dedicated proposed
Nina II (Daresbury)	ST	2.0	5.55	1000	3200	dedicated under construction
DCI (Orsay)	ST	1.8	3.82	400	3390	SR Lab
Phot-Fac (Japan)	ST	2.5	8		∿4300	dedicated, planned
Bonn II (Bonn)	SY	2.5	7.65	30	4530	SR Lab
Vepp 3 (Novosibirsk)	ST	2.5	6.15	∿100	5600	SR Lab
DORIS (Hamburg)	ST	3.5	12.12	500	7850	2 SR Labs
SPEAR (Stanford)	ST	4	12.7	60	11200	SR Lab
NINA I (Daresbury)	SY	5.0	20.8	50	13300	SR Lab
ARUS (Erewan)	SY	6.0	24.65	20	19500	SR Lab
DESY (Hamburg)	SY	7.5	31.7	30	25500	2 SR Labs
Group IV, $\varepsilon_c \geq$ 30 keV						
Cornell III (Ithaca)	SY	12	120	2	32000	SR Lab
EPIC	ST	14	172	22	35000	proposed
Pep (Stanford)	ST	15	170	100	44000	proposed
Petra (Hamburg)	ST	19	200	90	75000	under construction

Table II: VUV and soft x-ray radiation sources. For references, see Ref. 5, 28, 30, 37.; (a): monchromatized H_2 discharge

Source	Photon energy range [eV]	Linewidth	Remarks
He continuum	$12 \leq \hbar\omega \leq 21$	-	
Ne continuum	$12.4 \leq \hbar\omega \leq 16.8$	-	pressures of 50-200 torr
Ar continuum	$8 \leq \hbar\omega \leq 11.8$	-	
Kr continuum	$6.9 \leq \hbar\omega \leq 9.9$	-	
Xe continuum	$6.2 \leq \hbar\omega \leq 8.4$	-	
Hinteregger lamp[a]	$4 \leq \hbar\omega \leq 14$	multiline	
He I resonance lamp	21.2	∿1meV ?	
He II resonance lamp	40.8	<10meV	pressures of 0.1 - 0.5 torr
Ne I resonance lamp	16.8	∿1meV	
Ne II resonance lamp	26.9	<10meV?	
BRV Source	$4 \leq \hbar\omega \leq 250$	continuum and multiline	10^{-4} torr
YMξ x-rays	132.3	0.5 eV	
ZrMξ x-rays	151.4	0.8 eV	
NbMξ x-rays	171.4	1.2 eV	
RhMξ x-rays	260.4	4.0 eV	
TiMξ x-rays	452	-	
MgKα x-rays	1254	∿0.7 eV	
Al Kα x-rays	1487	∿0.8 eV	
Cu Kα x-rays	8055	∿2.5 eV	
DORIS (4 GeV)	$10^{-4} \leq \hbar\omega \leq 2\times10^{4}$	-	10^{-8} torr
DESY (7.5 GeV)	$10^{-4} \leq \hbar\omega \leq 3\times10^{4}$	-	10^{-6} torr

Table III. Survey on different types of grazing incidence monochromators used for SR experiments

TYPE	ACCELERATOR	NUMBER OF REFLECTIONS	GRATING	EXIT BEAM	RESOLUTION	REFERENCE
plane grating	DESY (Nowak et al.)	1	plane	moving	low	52
plane grating	INS-SOR (Miyake et al.)	2	plane	fixed	medium	52
plane grating	DESY (Kunz et al.)	3	plane	fixed	medium	58
plane grating	DNPL (West et al.)	2	plane	fixed	medium	53
spherical grating	Stanford/ Stoughton (Brown et al.)	4	spherical	fixed	medium	54
Rowland	all labs	2	spherical	moving	high	5
Rowland	Glasgow/DNPL (Codling et al.)	4	spherical	fixed	high	52
Rowland-Vodar	Stoughton (Pruett et al.)	3	spherical (two)	fixed	high	52
Rowland	Bonn (Thimm et al.)	2	spherical (two)	fixed	high	56
Rowland	ACO (Jaegle et al.)	5	spherical	fixed	medium	57
Rowland	INS-SOR (Sagawa et al.)	4	spherical	fixed	medium	57
parallel illumination	DESY (Haensel et al.)	1	spherical	moving	medium	52
distant source	NBS (Madden et al.)	1	toroidal	fixed	medium	52

Table IV Main areas of research with synchrotron radiation in atomic and molecular physics. Only a small selection of typical references is given.

GENERAL AREA	REFERENCES
Absorption cross sections	
rare gases	17,72
alkali- , alkaline earth atoms	74-77
atmospheric molecules	78,79
molecular alkali halides	80
polyatomic inorganic molecules	81
simple hydrocarbons	11
Photoelectron spectra, partial cross sections	
angular distributions, β parameters	82
energy dependence of partial cross sections	83
zero kinetic electron spectra	84
photoelectron spectra from the condensed phase	79
Fluorescence	
study of dissociative products	85
time resolved fluorescence	86
fluorescence from matrices, energy transfer	87
Mass spectroscopy	
fragmentation processes	88
supersonic beam experiments	89
Spectra from condensed gases	
atomic effects in solid state spectra	72,80,90
condensed gases, matrix isolation spectroscopy	17,79,91
organic molecular crystals	16,92

Table V Some of the main areas of research with synchrotron radiation in solid state physics. Only a small selection of typical references is given.

GENERAL AREA	REFERENCES
Bandstructure investigations	
absorption and reflection spectroscopy	10-18
modulation techniques	66-68
photoemission	18,71,106
Localized excitations	
Wannier-, Frenkel-, Core-Excitons	16-18,91,108
liegand field model	109
inner well states	90,110
Decay of excited states	
electron-electron scattering	114
relaxation of exciton states	87,111,112
energy-transfer processes	113
Surface Studies	
unoccupied surface states, surface excitons	115,116
electronic states of adsorbates	104
Many body effects	
intraatomic correlation effects	117
edge anomalies in simple metals	15,118,119

Table VI X-ray experiments with synchrotron radiation. Experiments marked by an asterik have been proposed but not yet performed.

EXPERIMENT	DESIRED INFORMATION	REFERENCES
EXAFS (absorption)	local structure	131,132
XPS (photoemission)	binding energies chemical shifts ħw dependence of cross sections surface studies	see chapter by H. Siegbahn in this book, 71
x-ray fluorescence	electronic band structure	134
Interferometry	real part of the forward scattering amplitude	32,63
Raman Scattering	accurate position of edges dispersion, linewidths	135
Compton Scattering		46,47
Small angle scattering	structure determination	34,62
Energy dispersive scattering	structure determination phase transitions	136,137
Topography	dislocations phase transitions	33,138,139,140
X-ray microscopy	observation of living cells element discriminating	64,141
X-ray lithography	structure information element discriminating	142, 143
Iodography* (Iodine absorption at I K-edge)	application medicine and biology, low iodine dose	
Standing wave impurity lattice location*	impurity lattice location information on surfaces	
Nonlinear and mixing with Lasers*		
Mössbauerspectroscopy*		

REFERENCES:

[1] LYMAN, T., "The Spectroscopy of the Extreme Ultraviolet", 2nd. ed., Longmans-Greene, New York (1928).

[2] DAMANY, N., ROMAND, J., VODAR, B., Eds., "Some Aspects of Vacuum Ultraviolet Radiation", Pergamon Press, Oxford (1974).

[3] KOCH, E.E., HAENSEL, R., KUNZ, C., Eds., "Vacuum Ultraviolet Radiation Physics", Vieweg-Pergamon, Braunschweig (1974).

[4] AZAROFF, L.V., Ed., "X-Ray Spectroscopy", McGraw-Hill, New York, (1974).

[5] SAMSON, J.A.R., "Techniques of Vacuum Ultraviolet Spectroscopy", Wiley, New York (1962).

[6] In astrophysics SR plays a major role. There exists a large number of papers dealing with the natural galactic and extra galactic SR-sources. For references, see Ref. 19.

[7] HARTMAN, P.L., TOMBOULIAN, D.H., Phys. Rev. 91, (1953) 1577, 102 (1958) 1423.

[8] HAENSEL, R., KUNZ, C., Z. Angew, Physik 23 (1967) 276.

[9] SOKOLOV, A.A., TERNOV, J.M., "Synchrotron Radiation", translated from the Russian, Pergamon Press, Oxford (1968).

[10] GODWIN, R.P., Springer Tracts in Mod. Phys., 51 (1969) 1.

[11] CODLING, K., Rep. Progr. Phys. 36 (1973) 541.

[12] BROWN, F.C., Solid State Physics 29 (1974) 1.

[13] MADDEN, R.P. in Ref. 4, p. 338.

[14] HAENSEL, R., Festkörperprobleme (1975) 203.

[15] KUNZ, C., in "Optical Properties of Solids-New Developments" (SERAPHIN, B.O., Ed.), North-Holland, Amsterdam-New York (1976) 473.

[16] KOCH, E.E., OTTO, A., Int. J. Radiat. Phys. Chem. 8 (1976) 113.

[17] SONNTAG, B., in "Rare Gas Solids" (KLEIN, M.L., VENABLES, J.A., eds.), Academic Press, New York (1976) in press.

[18] KOCH, E.E., KUNZ, C., SONNTAG, B., Reports in Physics, (1976) in press.

[19] MARR, G.V., MUNRO, I.M., SHARP, J.C.C., "Synchrotron Radiation, A Bibliography", Report DNPL/R24 (1972), Supplement DL/TM 127 (1974) Daresbury Nuclear Physics Laboratory.

[20] IWANENKO, D., POMERANCHUK, J., Phys. Rev. 65 (1944) 343.

[21] SCHWINGER, J., Phys. Rev. 70, (1946) 798, 75 (1949) 1912.

[22] See e.g., WATSON, G.N., "Bessel Functions", McMillan, New York (1945) p. 188.

[23] KOCH, E.E., KUNZ, C., WEINER, E.W., Optik 46 (1976) in press.

[24] KUNZ, C., Phys. Blätter 32, Jan. 1976.

REFERENCES CONT'D.

[25] BENARD, C., ROUSSEAU, M., J. Opt. Soc. Am. 64 (1974) 1433.

[26] KUNZ, C., in Ref. 3., p. 753.

[27] STEVENSON, J.R., ELLIS, H., BARTLETT, R., Appl. Optics 12 (1973) 2884.

[28] TANAKA, Y., JURSA, A.S., LEBLANK, F.J., J. Opt. Soc. Am. 48 (1958) 304.

[29] KOCH, E.E., Proc. 8th All Union Conf. of High Energy Particle Physics, Erevan April 1975, Vol. 2, Erevan (1976).

[30] See e.g. KINSINGER, J.A., STEBBINGS, W.L., VALENZI, R.A., TAYLOR, J.W., Anal. Chem. 44 (1972) 773.

[31] BALLOFFET, G., ROMAND, J., VODAR, B., C.R. Acad. Sci. (Paris) 252 (1961) 4139, and DAMANY, H., MEHLMAN, G., ROMAND, J. in Ref. 3, p. 720.

[32] BONSE, U., MATERLIK, G., in "Anomalous Scattering", RAMASESHAN, S., ABRAHAMS, S.C., Eds. Mungsgaard, Kopenhaben (1975) p. 107, and Hart, M., Bonse U. Phys. Today, Aug. 1970, p. 26.

[33] TUOMI, T., NAUKKARINEN, K., LAURILA, E., RABE, P., Acta Polytechnicy Scand. Ph-100 (1974).

[34] ROSENBAUM, G., HOLMS, K.C., WITZ, J. Nature 230 (1971) 434.

[35] EISENBERGER, P., Proc. Symp. Research Appl. of Synchrotron Radiation, Brookhaven Nat. Lab. Report 50-381 (1973), p. 70.

[36] SIEGBAHN, K., in "Electron Spectroscopy", SHIRLEY, D.A., Ed. North Holland, Amsterdam (1972) p. 31.

[37] KRAUSE, M.O., Chem. Phys. Letters 10 (1971) 65.

[38] ROWE, E.M., Private Communication, March (1976).

[39] Daresbury Laboratory Report DL/SFR/R2 (1975).

[40] See e.g. ROWE, E.M., MILLS, F.E., Particle Accelerators 4, (1973) 221.

[41] See e.g., WINICK, H., IEEE Trans. Nucl. Sci. NS 20 (1973) 984.

[42] KINCAID, B., Notes on the Second SSRP users meeting Stanford (1975) 52.

[43] ELIAS, L.R., FAIRBANK, W.M., MADEY, J.M.J., SCHWETTMAN, H.A., SMITH, T.J., Phys. Rev. Letters 36 (1976) 717.

[44] MOTZ, H., J. Appl. Phys. 42 (1971) 1906.

[45] MADEY, J.M.J., J Appl. Phys. 42 (1971) 1906.

[46] KUKIKOV, O.F., TELNOV, Y.Y., FILIPOV, E.I., YAKIMENKO, M.N., Phys Letters 13 (1964) 334.

[47] BEMPORAD, C., MILBURN, R.H., TANAKA, N., FOTINO, M., Phys. Rev. 138 B (1965) 1546.

[48] YEN, W.M., Optics Comm. 16 (1976) 5.

REFERENCES CONT'D.

[49] SKIBOWSKI, M., STEINMANN, W., J. Opt. Soc. Am. 57 (1967) 112.

[50] KOCH, E.E., SKIBOWSKI, M., Chem. Phys. Letters 9 (1971) 429.

[51] SAILE, V., SKIBOWSKI, M., STEINMANN, W., GÜRTLER, P., KOCH, E.E., KOZEVNIKOV, A., Submitted to Applied Optics and DESY report SR-76/05.

[52] KUNZ, C., in Proc. Intern. Symposium for Synchrotron Radiation Users, MARR, G.V., MUNRO, I.H., Eds. Daresbury Nuclear Phys. Lab. Report DNPL/R26 (1973) p.68.

[53] WEST, J.B., CODLING, K., MARR, G.V., J. Phys. E7 (1974) 137.

[54] BROWN, F.C., BACHRACH, R.Z., HAGSTROM, S.B.M., LIN, N., PRUETT, C.H., in Ref. 3, p. 785.

[55] THIMM, K., J. Electr. Spectr. 5 (1974) 755.

[56] JAEGLE, P., DHEZ, P., WUILLEUMIER, F., in Ref. 3, p. 788.

[57] SAGAWARA, H., SAGAWA, T., in Ref. 3, p. 790.

[58] DIETRICH, H., KUNZ, C., Rev. Sci. Instr., 43 (1972) 434.

[59] EBERHARDT, W., KALKOFFEN, G., KUNZ, C., to be published.

[60] BONSE, N., MATERCIK, G., SCHRODER, W., J. Appl. Cryst. (1976) in press.

[61] BEAUMONT, J.A., HART, M., J. Phys. E7 (1974) 823.

[62] BARRINGTON LEIGH, J., ROSENBAUM, G., J. Appl. Cryst. 7 (1974) 117.

[63] BONSE, U., MATERLICK, G., submitted to Phys. Rev. Letters.

[64] NIEMANN, B., RUDOLPH, D., SCHMAHL, G., Applied Optics (1976) in press.

[65] BACHRACH, R.Z., BROWN, F.C., HAGSTROM, S.B.M., J. Vac. Sci. Technol. 12 (1975) 309.

[66] OLSON, C.G., PIACENTINI, M., LYNCH, D.W., Phys. Rev. Letters 33 (1974) 644.

[67] ASPENES, D.E., OLSON, C.G., Phys. Rev. Letters 33 (1974) 1605.

[68] ASPENES, D.E., OLSON, C.G., LYNCH, D.W., Phys. Rev. B12 (1975) 2526.

[69] NIELSEN, U., DESY Report F41-74 March 1974.

[70] MADDEN, R.P., in "The Physics of Electronic and Atomic Collisions" RISLEY, J.S., GEBALLE, R., Eds. Seattle (1976) p. 568.

[71] EASTMAN, D.E., in Ref. 3, p. 417.

[72] CODLING, K., MADDEN, R.P., Phys. Rev. Letters 12 (1964) 106; HAENSEL, R., KEITEL, G., SHREIBER, P., KUNZ, C., Phys, Rev. 188 (1969) 1375.

[73] WOLFF, H.W., RADLER, K., SONNTAG, B, HAENSEL, R., Z. Phys. 257 (1972) 353; PETERSEN, H., RADLER, K., SONNTAG, B., HAENSEL, R., J. Phys. B8 (1975) 31.

REFERENCES CONT'D.

[74] MANSFIELD, M.W.D., CONNERADE, J.P., Proc. Roy. Soc. A342, (1975) 421.

[75] RABE, P., RADLER, K., WOLFF, H.W., in Ref. 3, p. 247.

[76] CONNERADE, J.P., MANSFIELD, M.W.D., Proc. Roy. Soc. A341 (1974) 267.

[77] EDERER, D.L., LUCATORTO, T.M., SALOMAN, E.B., MADDEN, R.P., AND SUGAR, J., J. Phys. B8 (1975) L21.

[78] CODLING, K., Astrophys. J. 143 (1966) 552; LEE, L.C., CARLSON, R.W., JUDGE, D.L., OGAWA, M., J. Quant. Spectr. Rad. Transfer 13 (1973) 1023.

[79] HIMPSEL, F.J., SCHWENTNER, N., KOCH, E.E., Phys. Stat. Sol. (b) 71 (1975) 615.

[80] RADLER, K., SONNTAG, B., CHANG, T.C., SCHWARZ, W.H.E., Chem. Phys. 13 (1976) 363; RADLER, K., SONNTAG, B., Chem. Phys. Letters 39 (1976) 371.

[81] HAYES, W., BROWN, F.C., Phys. Rev. 46 (1972) 21; COMES, F.J., HAENSEL, R., NIELSEN, U., SCHWARZ, W.H.E., J. Chem. Phys. 58 (1973) 576.

[82] HOULGATE, R.G., WEST, J.B., CODLING, K., MARR, G.V., J. Phys. B7 (1974) L470.

[83] GUSTUFSSON, T., PLUMMER, E.W., GUDAT, W., EASTMAN, W.E., to be published.

[84] JOCHIMS, H.W., LOHR, W., BAUMGARTEL, H., Ber. Bunsenges. Phys. Chem. 80 (1976) 130 and references therein.

[85] e.g., LEE, L.C., CARLSON, R.W., JUDGE, D.L., OGAWA, M. J. Chem. Phys. 63 (1975) 3987.

[86] LOPEZ-DELGADO, R., TRAMER, A., MUNRO, J.H., Chem. Phys. 5 (1974) 72; BENOISTD'AZY, O., LOPEZ-DELGADO, R., TRAMER, A., Chem. Phys. 9 (1975) 327.

[87] ACKERMANN, C., BRODMANN, R., HAHN, U., SUZUKI, A., ZIMMERER, G., Phys. Stat. Sol. (b) 74 (1976) in press.

[88] LOHR, W., JOCHIMS, H.W., BAUMGARTEL, H., Ber. Bunsenger. Phys. Chem. 79 (1975) 901.

[89] PARR, G.R., TAYLOR, J.W., J. Mass Spec. and Ion Phys. 14 (1974) 476.

[90] BLECHSCHMIDT, D., HAENSEL, R., KOCH, E.E., NIELSEN, U., SAGAWA, T., Chem. Phys. Letters 14 (1972) 33.

[91] PUDEWILL, D., HIMPSEL, F.J., SAILE, V., SCHWENTNER, N., SKIBOWSKI, M., KOCH, E.E., Phys. Stat. Sol. (b) (1976) in press.

[92] KOCH, E.E., OTTO, A., Chem. Phys. Letters 3 (1974) 370.

[93] SCHREIBER, P., Thesis Univ. Hamburg (1970).

[94] WENDIN, G., Phys. Letters 46A (1973) 119; and in Ref. 3, p. 225.

REFERENCES CONT'D.

[95] AMUSIA, M. YA., in Ref. 3, p. 205.

[96] EDERER, D.L., MANALIS, M., J. Opt. Soc. Am. 65 (1975) 634.

[97] COOPER, J.W., Phys. Rev. Letters 13 (1964) 762; FANO, U., COOPER, J.W., Rev. Mod. Phys. 40 (1968) 441.

[98] SAILE, V., GURTLER, P., KOZEVNIKOV, A., KOCH, E.E., to be published.

[99] KENNEDY, D.J., MANSON, S.T., Phys. Rev. A5 (1972) 227.

[100] KOCH, E.E., OTTO, A., Chem Phys. Letters 12 (1972) 476.

[101] KOCH, E.E., OTTO, A., RADLER, K., Chem. Phys. Letters 16 (1972) 131; 21 (1973) 501.

[102] EBERHARD, W., HAELBICH, R.-P, IWAN, M., KOCH, E.E., KUNZ, C., Chem. Phys. Letters (1976) in press.

[103] BAER, T., PEATMAN, W.B., SCHLAG, E.W., Chem. Phys. Letters 4 (1969) 243.

[104] GUSTAFSSON, T., PLUMMER, EE.W., EASTMAN, P.E., FREEOUF, J.L., Solid State Comm. 17 (1975) 371.

[105] HERTZ, H., JOCHIMS, H.W., SCHENK, H., SROKA, W., Chem. Phys. Letters 29 (1974) 572.

[106] GROBMAN, W., EASTMAN, D.E., FREEOUF, J.L., Phys. Rev. B12 (1975) 4405; GROBMAN, W., Comm. on Sol. State Phys. 7 (1975) 27.

[107] GUDAT, W., KUNZ, C., PETERSEN, H., Phys. Rev. Letters 32 (1974) 1370.

[108] OPHIR, Z., RAZ, B., JORTNER, J., SAILE, V., SCHWENTNER, N., KOCH, E.E., SKIBOWSKI, M., STEINMANN, W., J. Chem. Phys. 62, (1975) 650.

[109] ZIERAU, W., SKIBOWSKI, M., J. Phys. 68 (1975) 1671.

[110] FRIEDRICH, H., SONNTAG, B., RABE, P., SCHWARZ, W.H.E., to be published.

[111] ELIAS, L.R., HEAPS, W.S., YEN, W.M., Phys. Rev. B8 (1973) 4989.

[112] ONUKI, H., ONAKA, R., J. Phys. Soc. Jap. 34 (1973) 720.

[113] SCHWENTNER, N., KOCH, E.E., Phys. Rev. B (1976) in press.

[114] BAER, A.D., LAPEYRE, G.J., Phys. Rev. Letters 31 (1973) 1304; SCHWENTNER, N., to be published.

[115] EASTMAN, D.E., FREEOUF, J.L., Phys. Rev. Letters 33 (1974) 1601; LAPEYRE, G.J., ANDERSON, J., Phys. Rev. Letters 35 (1975) 117.

[116] SAILE, V., SKIBOWSKI, M., STEINMANN, W., GURTLER, P., KOCH, E.E., KOZEVNIKOV, A., submitted to Phys. Rev. Letters.

[117] HAENSEL, R., RABE, P., SONNTAG, B., Sol. State Comm. 8 (1970) 1845.

[118] PETERSEN, H., KUNZ, C., Phys. Rev. Letters 35 (1975) 863.

[119] PETERSEN, H., Phys. Rev. Letters 35 (1975) 1363; see also KUNZ, C., PETERSEN, H., LYNCH, D.W., Phys. Rev. Letters 33 (1974) 1556.

REFERENCES CONT'D.

[120] FESER, K., Phys. Rev. Letters 28 (1972) 1013.

[121] LAPEYRE, G.J., BAER, A.D., HERMANSON, J.C., ANDERSON, J., KNAPP, J.A., GOBBY, D.L., Sol. State Comm. 15 (1974) 1601.

[122] CARDONA, M., GUDAT, W., KOCH, E.E., SKIBOWSKI, M., SONNTAG, B., YU, P.Y., Phys. Rev. Letters 25 (1970) 659.

[123] SCHWENTNER, N., HIMPSEL, F.J., SAILE, V., SKIBOWSKI, M., STEINMANN, W., KOCH, E.E., Phys. Rev. Letters 34 (1975) 528.

[124] EASTMAN, D.E., FREEOUF, J.L., Phys. Rev. Letters 34 (1975) 395.

[125] HIMPSEL, F.J., STEINMANN, W., Phys. Rev. Letters. 35 (1975) 1025.

[126] KUNZ, C., HAENSEL, R., KEITEL, G., SCHREIBER, P., SONNTAG, B., in: NBS Spec. Publ. 323, Washington (1971) p. 275, BENNETT, L.H., Ed.

[127] HAENSEL, R., KEITEL, G., SCHREIBER, P., SONNTAG, B., KUNZ, C., Phys. Rev. Letters 23 (1969) 528.

[128] MAHAN, G.D., Phys. Rev. 153 (1967), 882; 163 (1962) 612; Solid State Phys, 29 (1974) 75.

[129] NOZIERES, P., DEDOMINICIS, C.T., Peys. Rev. 176 (1969) 1092.

[130] e.g., DOW, J.D., ROBINSON, J.E., SLOWIK, J.H., SONNTAG, B.F., Phys. Rev. B10 (1974) 432.

[131] KINCAID, B.M., EISENBERGER, P., Phys. Rev. Letters 34 (1975) 1361.

[132] See for instance: KINCAID, B.M., EISENBERGER, P., HODGSON, K.O., DOMACH, S., Proc. Nat. Acad. Sci, USA, 72 (1975) 2340; STERN, E.A., Phys. Rev. B10 (1974) 3027; ASHLEY, C.A., DOMACH, S., Phys Rev. B11 (1975) 1279; STERN, E.A., Scientific American 234, April 1976, 96.

[133] AZAROFF, I., Rev. Mod. Phys. 35 (1963) 1012.

[134] MULLER, J., FESER, K., WIECH, G., FAESSLER, A., Phys. Letters 44A (1973) 263.

[135] EISENBERGER, P., PLATZMANN, P.M., WINICK, H., Phys. Rev. Letters, 36 (1976) 623.

[136] BORDAS, J., GLAZER, M., MUNRO, I.H., Submitted to Nature (1976)

[137] BURAS, B., STAUN OLSEN, J., GERWARD, L., Nucl. Instr. and Methods (1976) in press.

[138] TUOMI, T., NAUKKARINEN, K., RABE, P., Phys. Stat. Soc. (a) 25 (1974) 93.

[139] HART, M., J. Appl. Crystallogr. 8 (1975) 436.

[140] BORDAS, J., GLAZER, A.M., HAUSER, H., Phil. Mag. 32 (1975) 471.

[141] HOROWITZ P., HOWELL, J.A., Science 178 (1972) 608.

[142] SPILLER, E., FEDER, R., TOPALIAN, J., EASTMAN, D.E., GUDAT, W., SAYER, D., Science 191 (1976) 1172.

[143] SPILLER, E., FEDER, R., TOPALIAN, J., GUDAT, W., EASTMAN, D.E., IBM Research Note 25 123, Jan. 1976.

REFERENCES CONT'D.

[144] GIESSEN, B.C., GORDON, G.E., Science 159 (1968) 973.

[145] SCHMAHL, G., in Ref. 3, p. 667.

[146] NIEMANN, B., RUDOLPH, D., SCHMAHL, G., Optics Comm. 12 (1974) 160.

[147] AOKI, S., ICHIHARA, Y., KIKUTA, S., Jap. J. Appl. Phys. 11 (1972) 1857.

[148] HOLMES, K.C., in Ref. 3, p. 809.

[149] HAGEMANN, H.J., GUDAT, W., KUNZ, C., J. Opt. Soc. Am., 65 (1975) 742, and DESY Report SR-74/7.

[150] HAELBICH, R.P., KUNZ, C., Optics Comm. (1976), in press.

[151] LEMKE, D., LABS, D., Appl. Opt. 6 1043 (1967); PITZ, E., Appl. Opt. 8 (1969) 255; STUCK, D., WENDE, B., J. Opt. Soc. Am. 52 (1972) 96.

[152] KEY, P.J., Metrologica 6 (1970) 97.

[153] SIPP, B., MICHE, J.A., LOPEZ-DELGADO, R., Opt. Comm. 16 (1976) 202.

FIGURE CAPTIONS

Fig. 1. Applications of Synchrotron radiation in basic and applied research. The various spectral ranges and spectroscopic techniques are indicated.

Fig. 2. A sketch of the history of synchrotron radiation as a research tool. For references, see Ref. 8,9, and 13.

Fig. 3. Spectral distribution of synchrotron radiation into a solid angle of 1mradx 1mrad for DORIS at different operating conditions. For comparison a curve typical for the DESY synchrotron is given (from Ref. 23).

Fig. 4. Geometry of synchrotron radiation emission. The plane of the accelerator or storage ring is filled with radiation (top) while the intensity in the off plane direction drops rapidly with increasing angle ψ (bottom) from Ref. 29.

Fig. 5. Angular distribution of intensity components with electrical vector parallel (I_{11}) and normal ($I_{\perp}$) to the plane of the synchrotron, linear polarization, and circular polarization (from decomposition into left (I_L) and right (I_R) hand circularly polarized components) for the DORIS storage ring calculated for three photon energies $\hbar\omega$. ψ is the elevation angle perpendicular to the orbital plane (from Ref. 24).

Fig. 6. The DESY synchrotron and DORIS storage rings at Hamburg. There are four synchrotron radiation laboratories L1 to L4. Laboratories 1 and 3 are used by various groups for VUV and x-ray experiments. Laboratories 2 and 4 are used for x-ray diffraction experiments on biological objects by the European Molecular Biology Laboratory (EMBL).

Fig. 7. Schematic spectral distribution of synchrotron radiation with the electron energy in GeV as a parameter. The spectra of rare gas discharge lamps (Ref. 28) are shown for comparison (from Ref. 29).

Fig. 8. Spectral distribution of intensity into a 2 cm x 2cm wide aperture at laboratory distance d at different accelerators and storage rings (from Ref. 26).

Fig. 9. Brightness of synchrotron radiation from DORIS (source size 1x10mm^2), DESY (source size 3x10mm^2), Cu K_α characteristic radiation and bremsstrahlung from a 60 KW x-ray tube [36] (estimated source size 2mm diameter) and the He,I (21.2 eV) resonance line [30] (estimated source size 10 mm diameter, 20 meV line width, guessed collimation of the quoted 10^{13} photons into 0.01 sterad) (from Ref. 26).

Fig. 10. Principle of a wavelength shifter and a wiggler device.

Fig. 11. Block diagram showing the various instrumental aspects of VUV-spectroscopy with synchrotron radiation (from Ref. 29).

FIGURE CAPTIONS CONT'D.

Fig. 12. Optical layout of the synchrotron radiation beam lines at the synchrotron radiation laboratory at DORIS. The beam (from left) is split into four independent beams, L_1, L_2, D and R. S_1 to S_4, plane mirrors, FM, focusing mirrors; FG, concave reflectance gratings; G, grating; Mi, flat mirrors; SL entrance and exit slits respectively, FL, x-ray fluorescence experiment, x-ray/row, space for an x-ray experiment or a Rowland monchromator (from Ref. 23).

Fig. 13. Schematic drawing of the beam pipe and the 3 m normal incidence monochromator cut perpendicular to the storage ring plane. Synchrotron radiation (SR) enters from the left, is deflected 15° out of its direction by a plane mirror in the mirror chamber PCM and reflected upwards 15° and focused by the toroidal mirror TM in the TM-chamber TMC onto the entrance slit (S) of the monochromator (225.3 D). It hits the grating (G). A monochromatic beam emerges horizontally from the exit slit (S) into the experimental chamber (EC). V - valve (from Ref. 51).

Fig. 14 Layout of the grating incidence monochromator built by Dietrich and Kunz. Units I and II are vibrationally isolated from the vacuum housing. They sit on separate supports and are decoupled by soft bellows B. A_1 and A_2, beam apertures; M, premirrors; G, grating; F, focusing mirror; S, exit slit; Fi, thin film filters; MP, open photomultiplier; GP and TMP, pumping system (from Ref. 58).

Fig. 15. Top view and side view of the remotely controlled optical bench in the EMBL laboratory at DESY for x-ray diffraction on biological specimens (after Ref. 62).

Fig. 16. Absorption of gaseous (g) and solid (f) Krypton in the photon energy range from 9 to 600 eV (from Ref. 93).

Fig. 17. 4 d absorption spectrum of atomic and solid barium and calculated relative oscillator strengths of 4d → 4f, 5f, and 6p transitions (from Ref. 75).

Fig. 18. Structure in the photoionization continuum of Xenon due to transitions $4d^{10}\ 5s^2\ 5p^6 \rightarrow 4d^9\ 5s^2\ 5p^6 np$ (from Ref. 96).

Fig. 19. Absorption spectrum of Krypton in the range between the first and second ionization potential (Beutler-Funo resonances) with high resolution. The two p→s and p→d series interact with each other and with the underlying continuum (from Ref. 98).

Fig. 20. Electron yield spectra of gaseous ethylene, benzene and acetylene in the range of the C ls absorption. Photon energies of the peak positions and the ionization potentials are given for each spectrum (from Ref. 102).

Fig. 21. Resonant photoelectron spectra of CF_3Cl, CF_2Cl_2 and $CFCl_3$ (after Ref. 84).

FIGURE CAPTIONS CONT'D

Fig. 22. Relative photoionization yield curves of NO; (a) NO^+; (b) O^+ and (c) N^+ (from Ref. 105).

Fig. 23. Absorption of crystalline and amorphous GaP (upper part, after Ref. 122) and Schottky-barrier electroflectance spectrum of GaP at 80K (lower part, after Ref. 68) (from Ref. 18).

Fig. 24. Photoelectron energy distribution curves for solid Ne, Ar, Kr, and Xe for various photon energies below the onset of electron-electron scattering (from Ref. 123).

Fig. 25. Photoelectron energy distribution curves for NiO. The zero of the energy is placed at the d-state peak and the arrows E_E, E_D and E_P are the fermi energy, d-state energy and p-band edge. Partial d-state emission intensities (dashed lines) and p-band intensities (broken lines) are shown (from Ref. 124).

Fig. 26. Polar diagram of the photoemission intensity as a function of azimuth Ø for KCl (100) face at a fixed polar angle Θ of 45° for three final energies (15, 16, and 18 eV above the top of the valence band) and two initial energies (Cl^- 3p valence band and K^+ 3p core level) (10) marks the orientation in which the (10) surface vector lies in the emission plane (from Ref. 125).

Fig. 27. The Li ls absorption edge [126] and the Na 2p absorption edges [127] (from Ref. 18).

Fig. 28. Principle of the energy-dispersive x-ray method using synchrotron radiation. 2Θ, fixed scattering angle; S_1 and S_2, slits; A, focus point; D, semiconductor detector; MCA, multichannel pulse-height analyser (from Ref. 137).

Ref. 29. Energy dispersive diffraction spectrum of Iron powder recorded with a Ge detector; Slit widths are given for S_1 and S_2; ec, escape peaks. In addition to the diffraction lines, some fluorescence lines are seen (from Ref. 137).

Fig. 30. A $2\bar{2}0$ transmission (Guinier-Temerin) topograph of a 0.3 mm thick silicon crystal. The maximum electron energy of the synchrotron was 6 GeV and the current was 7mA. The exposure time was 8 sec. (from Ref. 138).

Fig. 31 Experimental arrangement for the x-ray zone-plate microscope (from Ref. 64).

Fig. 32. Test picture of a wire mesh taken with the zone-plate microscope. The resolution is about 0.5 µm. (B. Niemann, unpublished).

Fig. 33. Principle of x-ray micrography. (a) Irradiation of the x-ray resist through the specimen. In x-ray lithography, the specimen is a mask generated by an electron beam. (b) the replica after development of the resits (from Ref. 142).

Fig. 34. X-ray replicas of diatoms obtained with synchrotron radiation (c) is a detail of (b) (from Ref. 143).

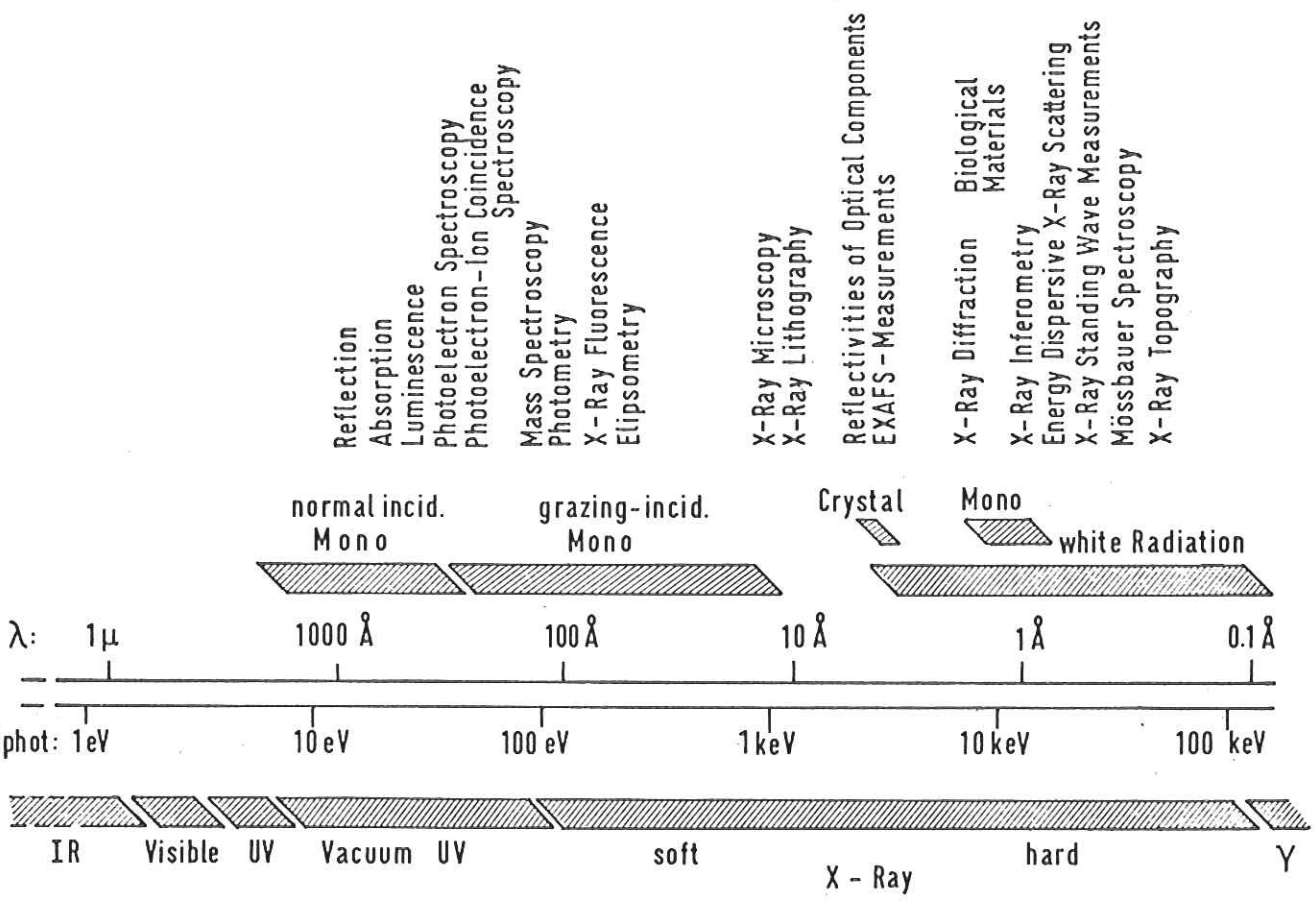
Reflection
Absorption
Luminescence
Photoelectron Spectroscopy
Photoelectron-Ion Coincidence Spectroscopy
Mass Spectroscopy
Photometry
X-Ray Fluorescence
Elipsometry
X-Ray Microscopy
X-Ray Lithography
Reflectivities of Optical Components
EXAFS-Measurements
X-Ray Diffraction
Biological Materials
X-Ray Inferometry
Energy Dispersive X-Ray Scattering
X-Ray Standing Wave Measurements
Mössbauer Spectroscopy
X-Ray Topography
normal incid. Mono
grazing-incid. Mono
Crystal
Mono
white Radiation
λ: 1μ 1000 Å 100 Å 10 Å 1 Å 0.1 Å
Ephot: 1eV 10 eV 100 eV 1 keV 10 keV 100 keV
IR
Visible
UV
Vacuum UV
soft
X - Ray
hard
γ

Fig. 1

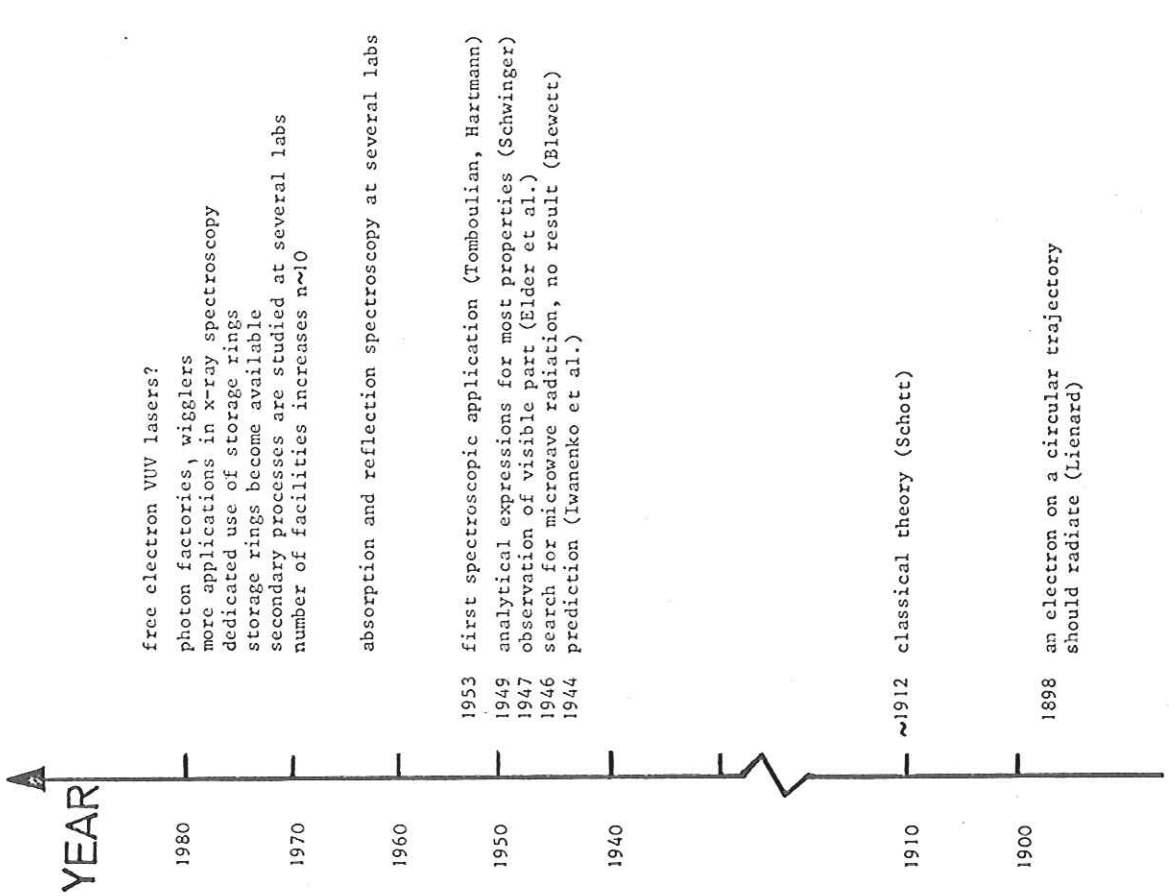
YEAR
1980
1970
1960
1950
1940
1910
1900
free electron VUV lasers?
photon factories, wigglers
more applications in x-ray spectroscopy
dedicated use of storage rings
storage rings become available
secondary processes are studied at several labs
number of facilities increases n~10
absorption and reflection spectroscopy at several labs
1953 first spectroscopic application (Tomboulian, Hartmann)
1949 analytical expressions for most properties (Schwinger)
1947 observation of visible part (Elder et al.)
1946 search for microwave radiation, no result (Blewett)
1944 prediction (Iwanenko et al.)
~1912 classical theory (Schott)
1898 an electron on a circular trajectory should radiate (Lienard)

Fig. 2

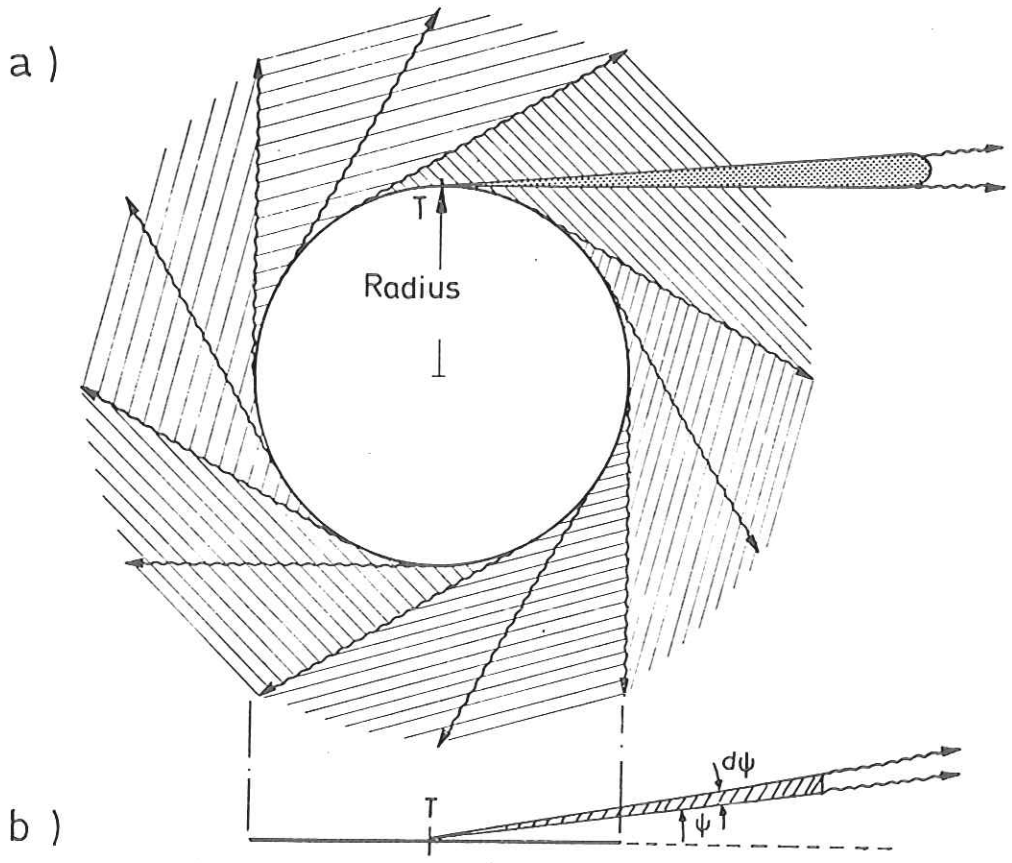

DESY

24703

Fig. 4

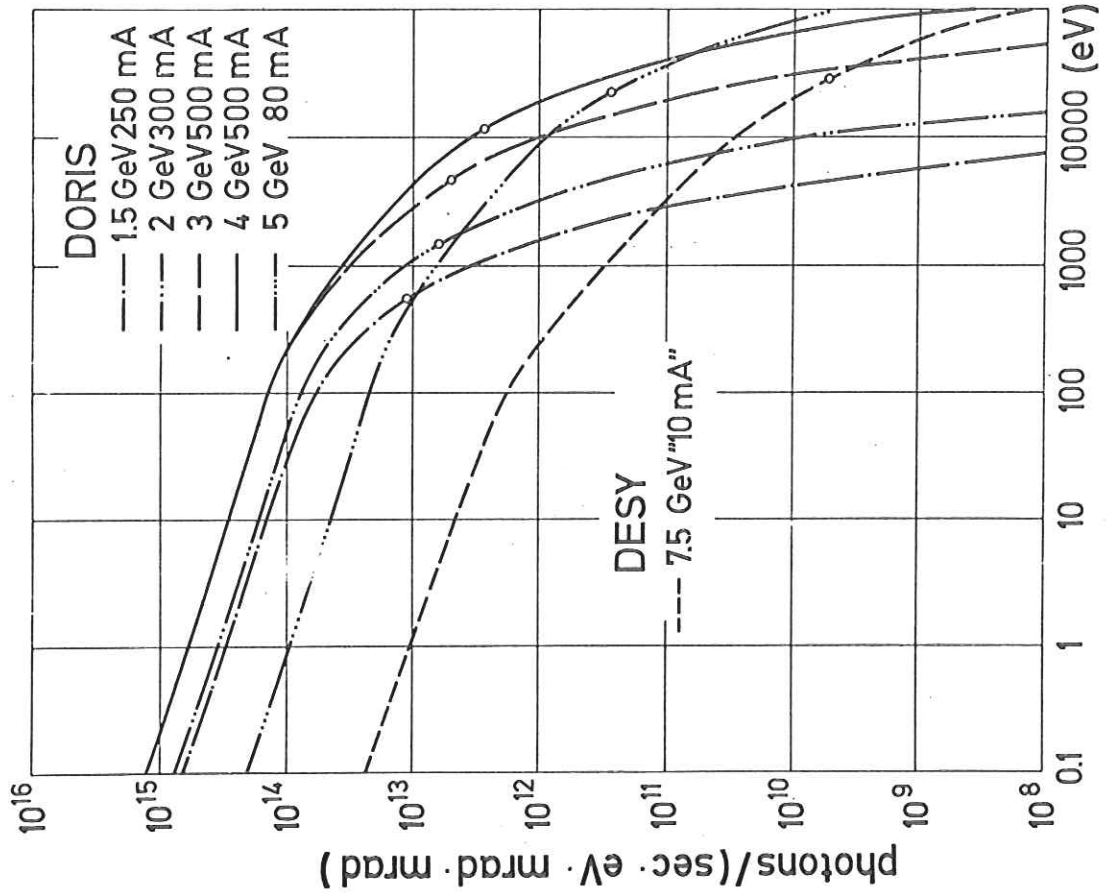

Fig. 3

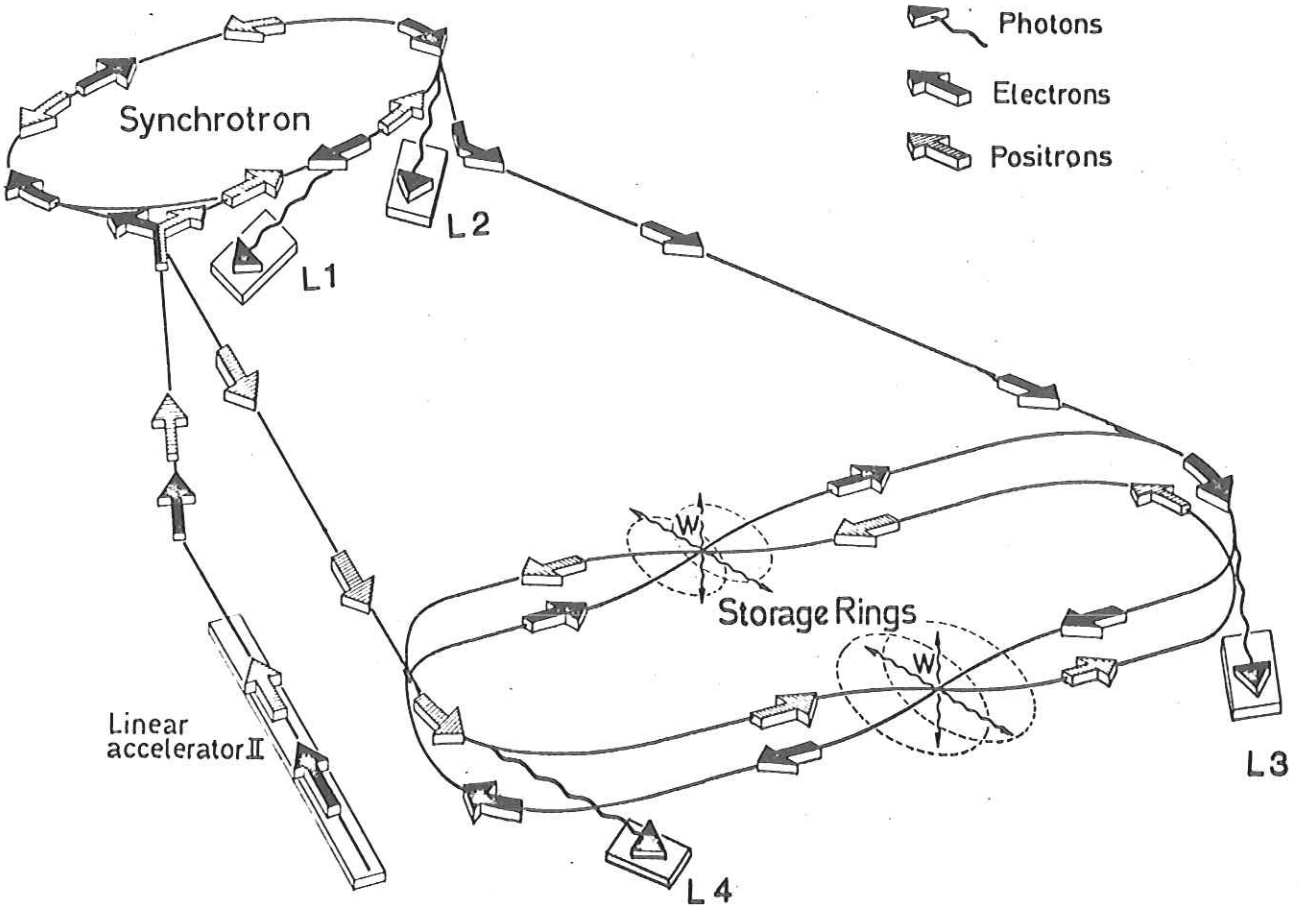
Photons
Electrons
Positrons
Synchrotron
L1
L2
L3
L4
W
W
Storage Rings
Linear
accelerator II

Fig. 6

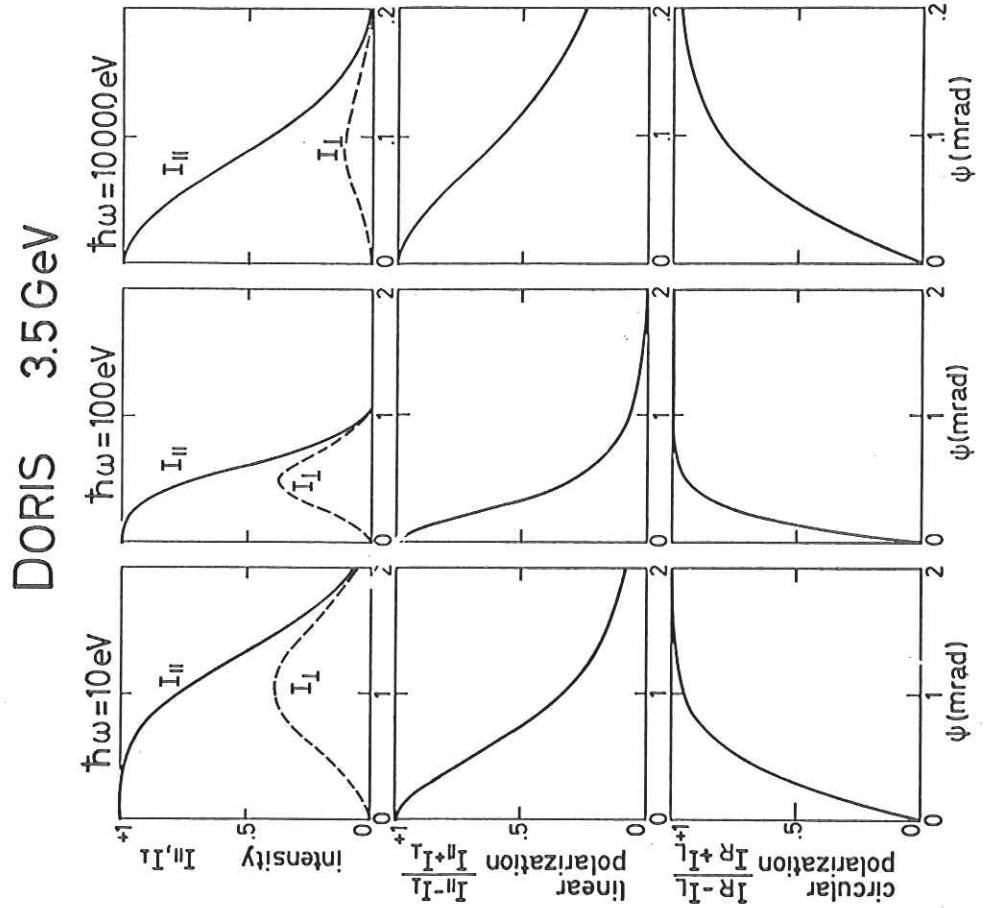
DORIS 3.5 GeV
ħω=10 eV
ħω=100 eV
ħω=10000 eV
I∥
I⊥
intensity I∥,I⊥
linear polarization (I∥-I⊥)/(I∥+I⊥)
circular polarization (IR-IL)/(IR+IL)
ψ (mrad)

Fig.5

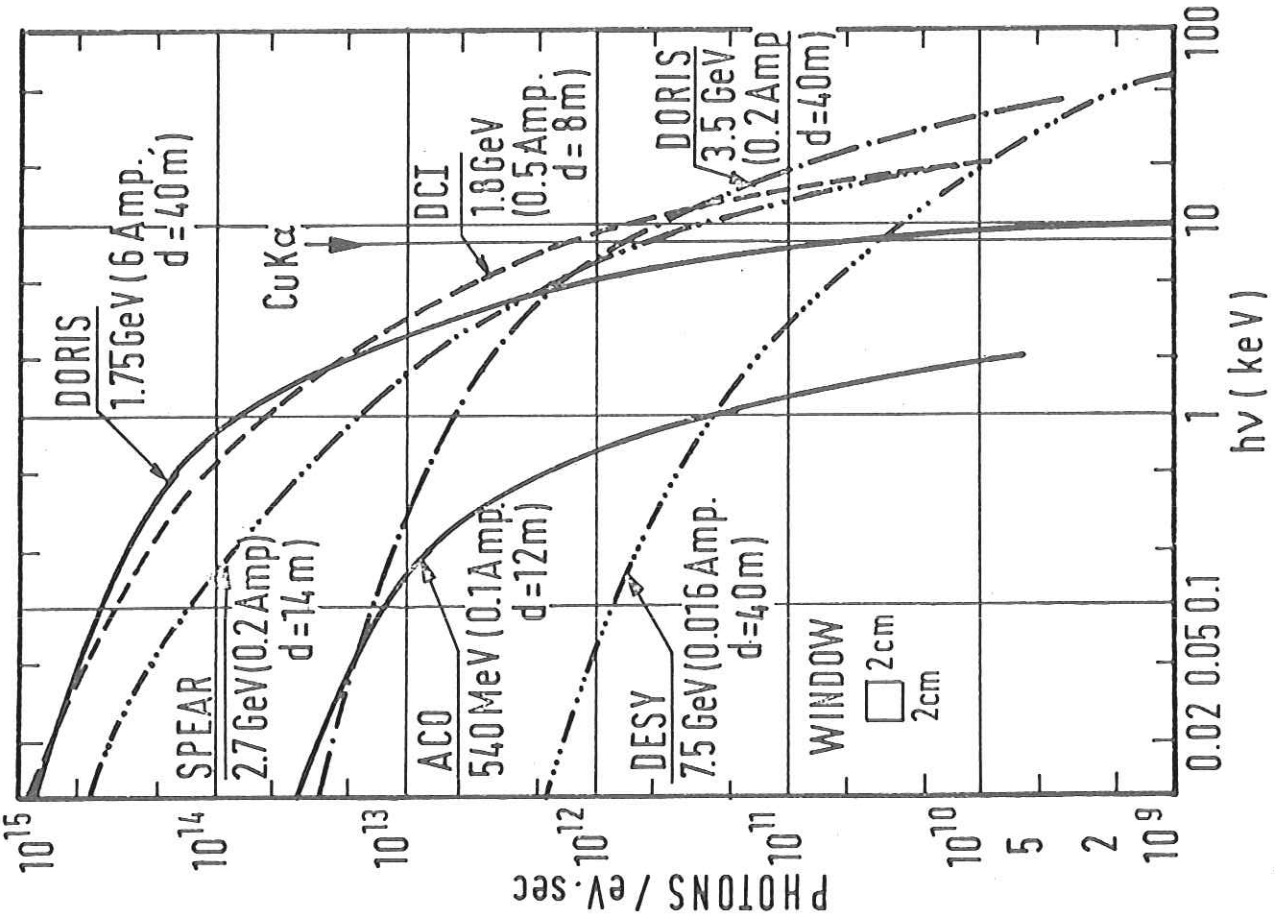
DORIS
1.75GeV (6 Amp. d=40m)
SPEAR
2.7GeV (0.2 Amp) d=14m)
CuKα
DCI
1.8GeV (0.5 Amp. d=8m)
ACO
540 MeV (0.1 Amp. d=12m)
DORIS
3.5 GeV (0.2 Amp d=40m)
DESY
7.5 GeV (0.016 Amp. d=40m)
WINDOW
2cm
2cm
PHOTONS / eV.sec
hν (keV)

Fig. 8

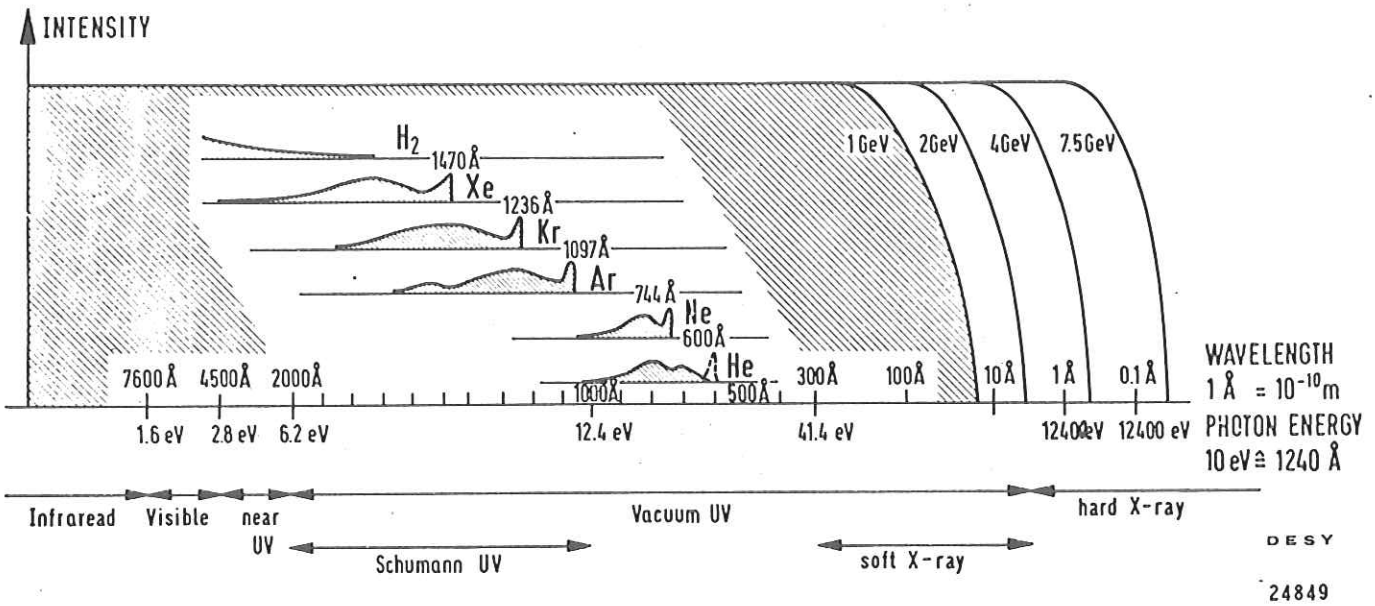
INTENSITY
H2 1470Å
Xe 1236Å
Kr 1097Å
Ar 744Å
Ne 600Å
He 500Å
1000Å
1 GeV
2GeV
4GeV
7.5GeV
7600Å 4500Å 2000Å
300Å
100Å
10Å
1Å
0.1Å
WAVELENGTH
1 Å = 10⁻¹⁰m
1.6 eV 2.8 eV 6.2 eV
12.4 eV
41.4 eV
12400eV 12400 eV
PHOTON ENERGY
10 eV ≙ 1240 Å
Infraread
Visible
near UV
Vacuum UV
hard X-ray
Schumann UV
soft X-ray
DESY
24849

Fig. 7

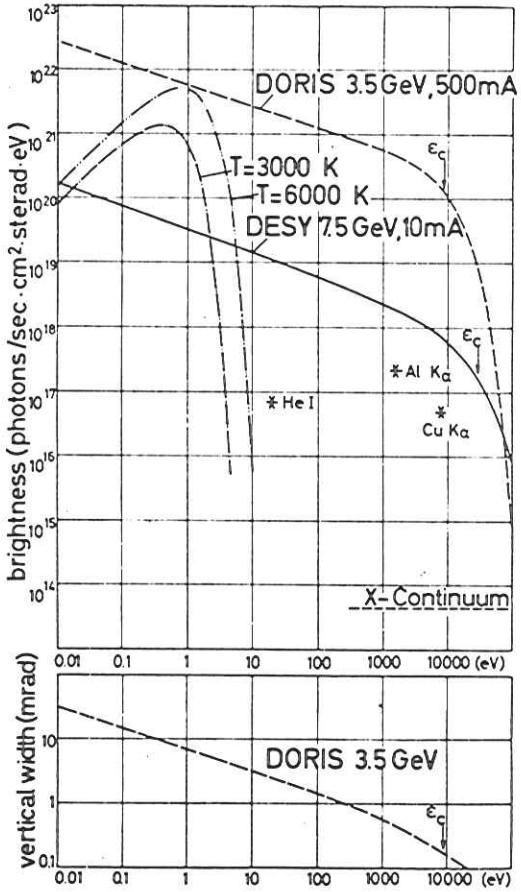

Fig. 9

WAVELENGTH SHIFTER

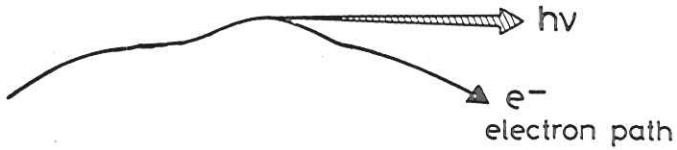

MULTIPOLE WIGGLER MAGNET

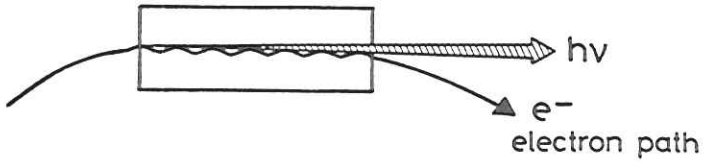

Fig. 10

SOURCE	ACESS	MONOCHROMATORS	EXPERIMENT
Accelerators Storage Rings Wigglers	Radiation Beam Lines Mirrors Vacuum Requirements Safety	Normal Incidence Monochromators Grazing Incidence Monochromators Crystal Spectrometers X-Ray Interferometers Grating Technology	Detectors Absorption Cells Molecular Beams Reflectometers Photoelectron Analyzers Secondary Monochremators Mass Filters Modulation Devices Electronics Data Acquisiton Systems

Fig.11

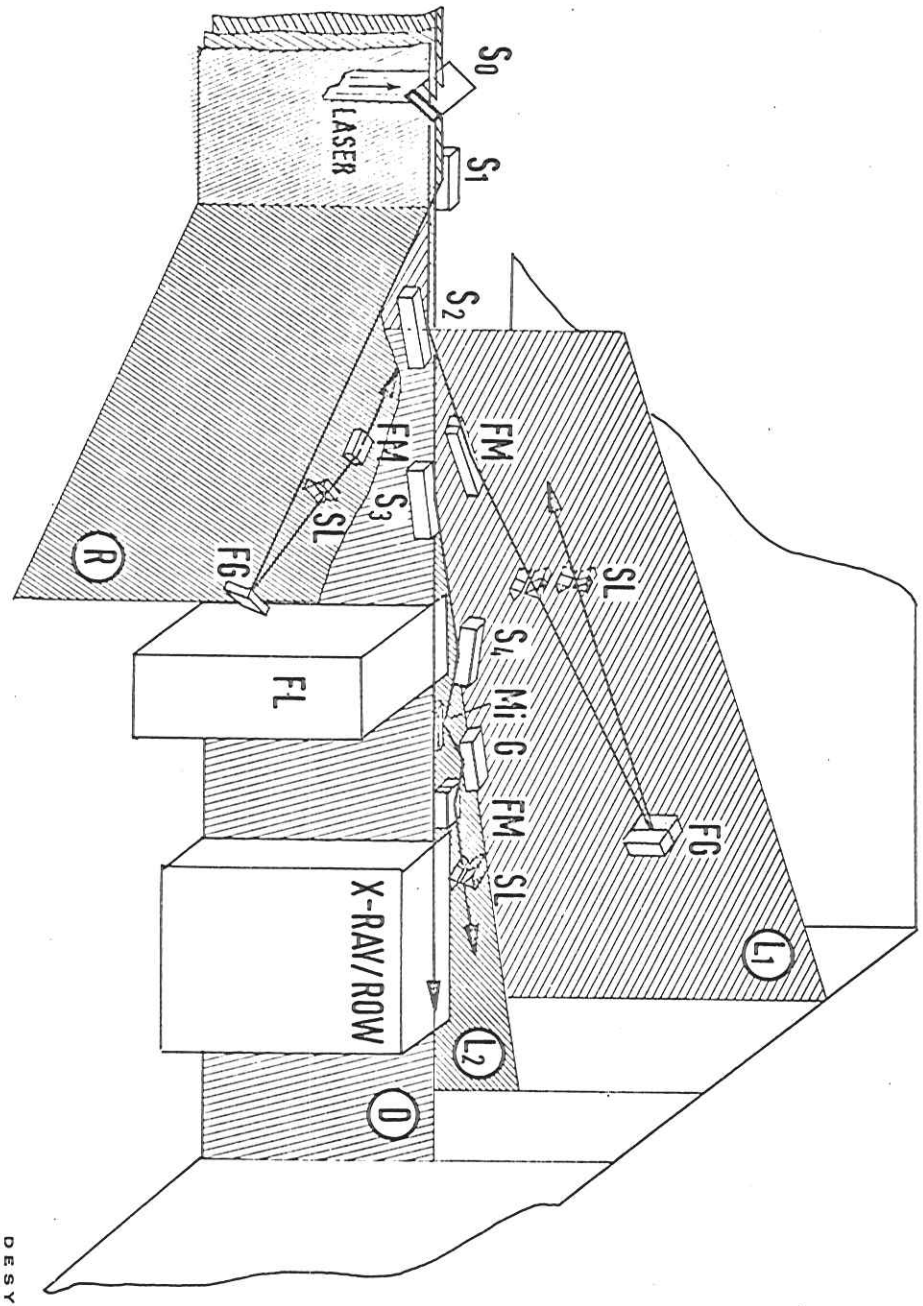

Fig.12

DESY
24137

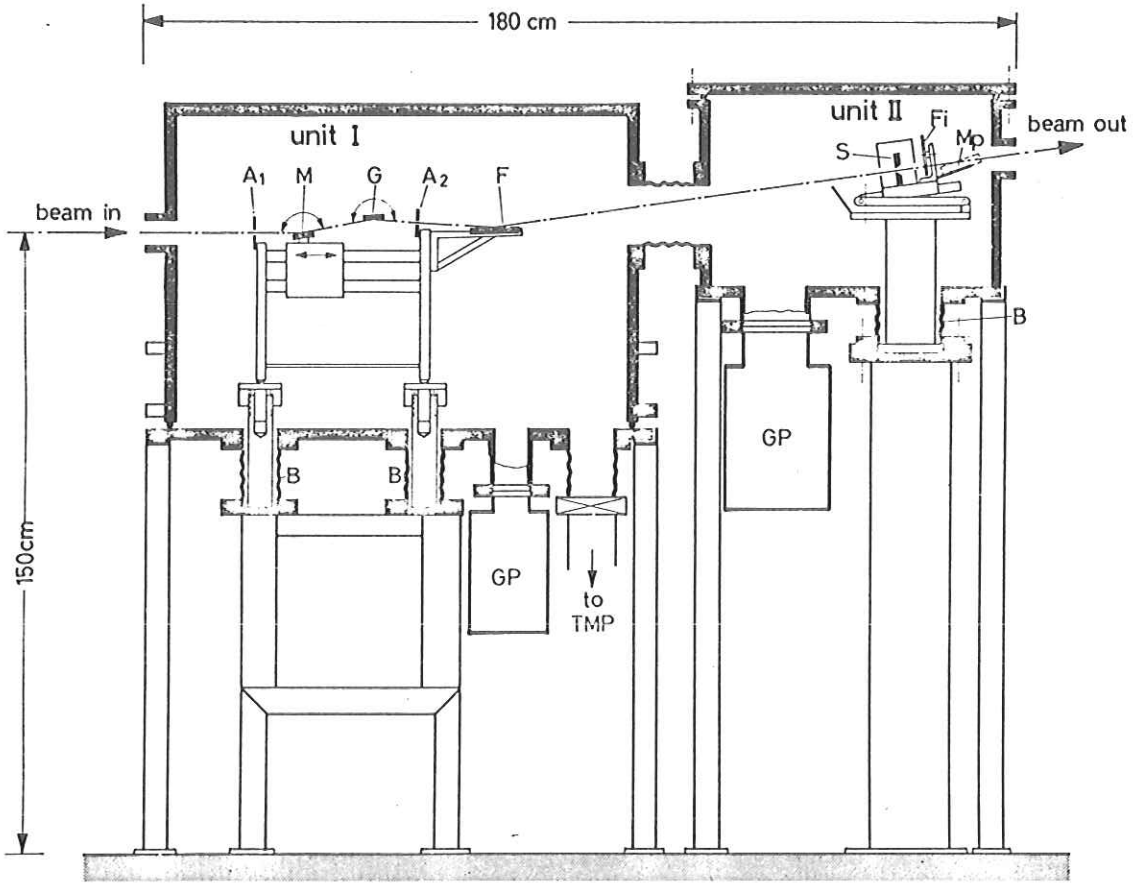
180 cm
unit I
unit II
beam in
beam out
A1
M
G
A2
F
Fi
S
Mp
B
B
B
GP
GP
to
TMP
150cm

Fig.14

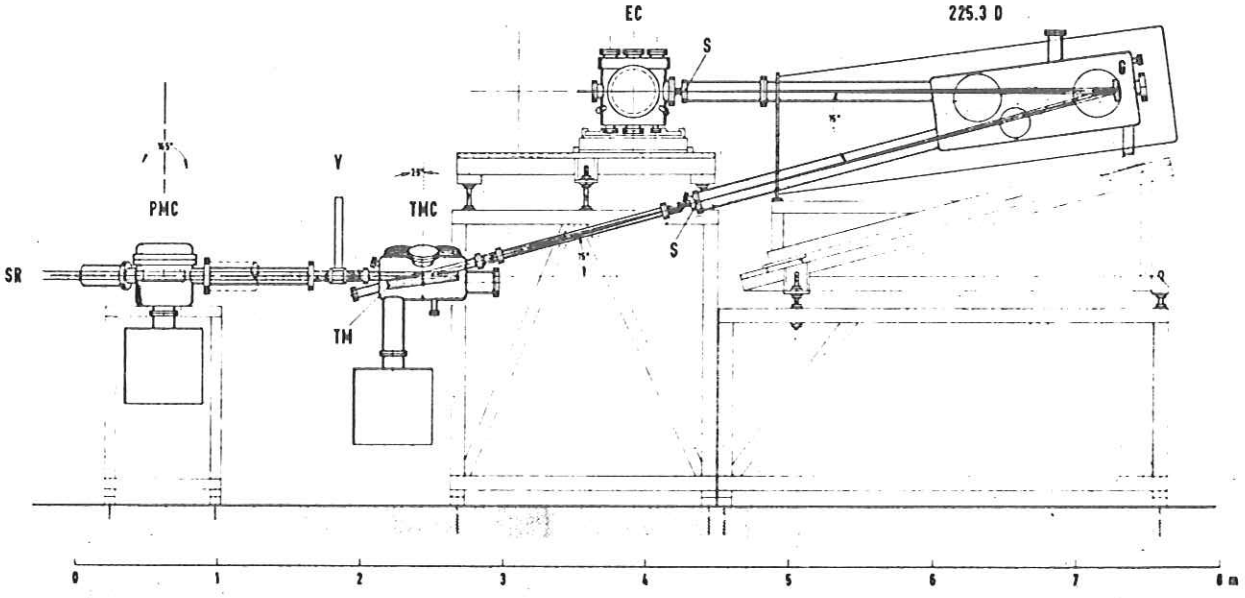
EC
225.3 D
S
G
PMC
V
THC
S
SR
TH
0
1
2
3
4
5
6
7
8 m

Fig.13

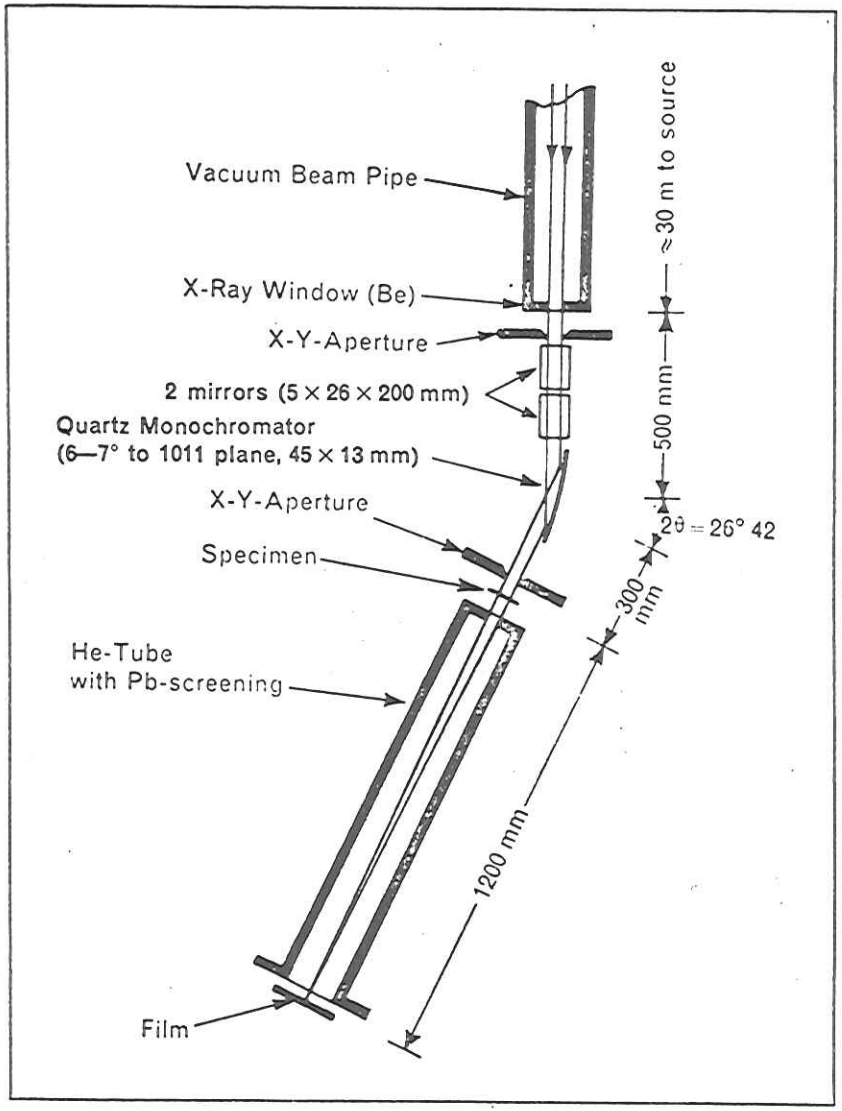
Vacuum Beam Pipe
X-Ray Window (Be)
X-Y-Aperture
2 mirrors (5 × 26 × 200 mm)
Quartz Monochromator
(6—7° to 1011 plane, 45 × 13 mm)
X-Y-Aperture
Specimen
He-Tube
with Pb-screening
Film
≈ 30 m to source
500 mm
2ϑ = 26° 42
300 mm
1200 mm

Fig.15

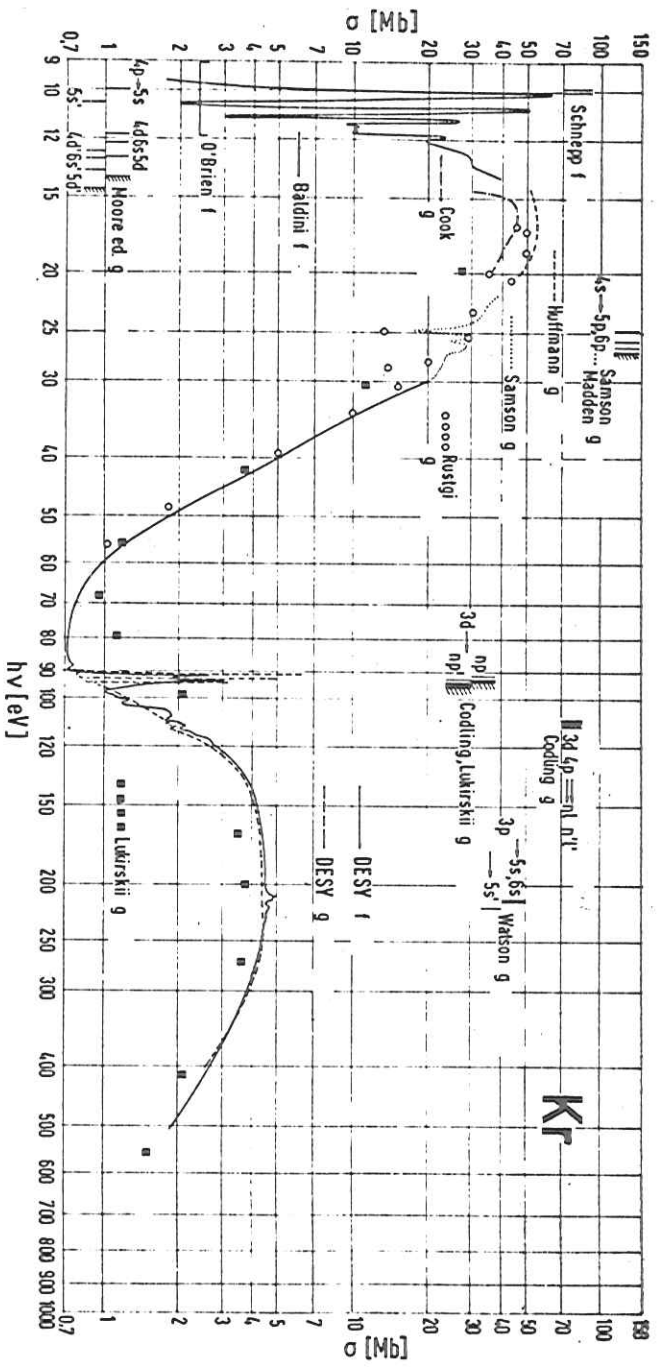
σ [Mb]
hν [eV]
Kr
Schnepp f
O'Brien f
Baldini f
Cook g
Hoffmann g
Samson g
Rustgi g
Hudden g
Moore ed. g
Codling, Lukirskii g
Codling g
Lukirskii g
DESY f
DESY g
Watson g

Fig.16

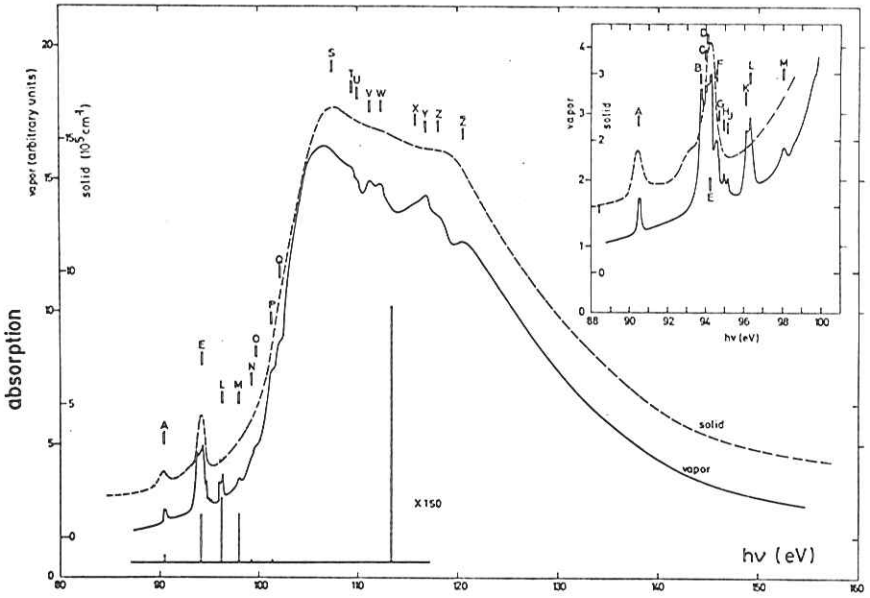
absorption
vapor (arbitrary units)
solid (10^5 cm^{-1})
A
E
L M
N
O
P
Q
S
T U
V W
X Y Z
Z
X150
solid
vapor
hν (eV)
vapor
solid
A
B
C
D
E
F
L
M
hν (eV)

Fig.17

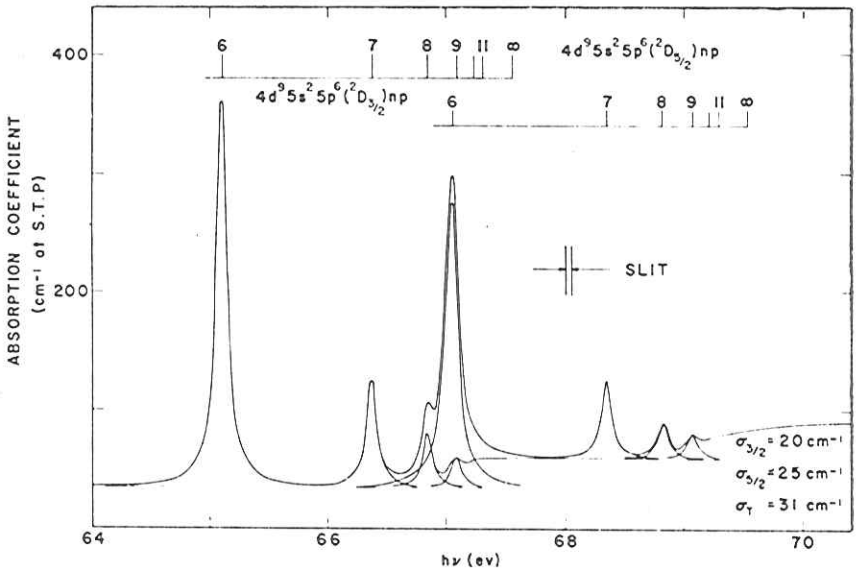
ABSORPTION COEFFICIENT
(cm^{-1} at S.T.P)
400
200
6
7
8
9
11
∞
$4d^9 5s^2 5p^6 (^2D_{5/2}) np$
$4d^9 5s^2 5p^6 (^2D_{3/2}) np$
SLIT
$\sigma_{3/2}$ = 20 cm^{-1}
$\sigma_{5/2}$ = 25 cm^{-1}
σ_T = 31 cm^{-1}
64
66
68
70
hν (ev)

Fig.18

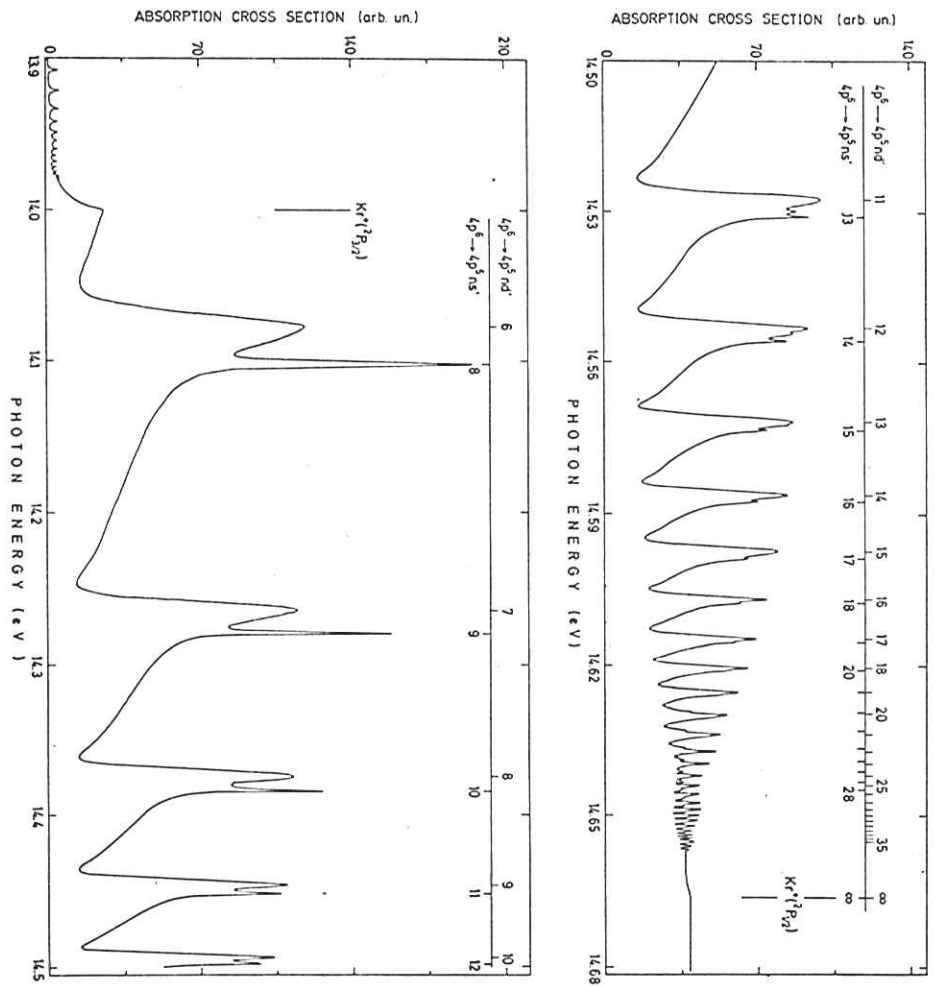
ABSORPTION CROSS SECTION (arb. un.)
PHOTON ENERGY (eV)
$Kr^+(^2P_{3/2})$
$4p^6 \rightarrow 4p^5 nd'$
$4p^6 \rightarrow 4p^5 ns'$
ABSORPTION CROSS SECTION (arb. un.)
PHOTON ENERGY (eV)
$Kr^+(^2P_{3/2})$
$4p^6 \rightarrow 4p^5 nd'$
$4p^6 \rightarrow 4p^5 ns'$

Fig. 19

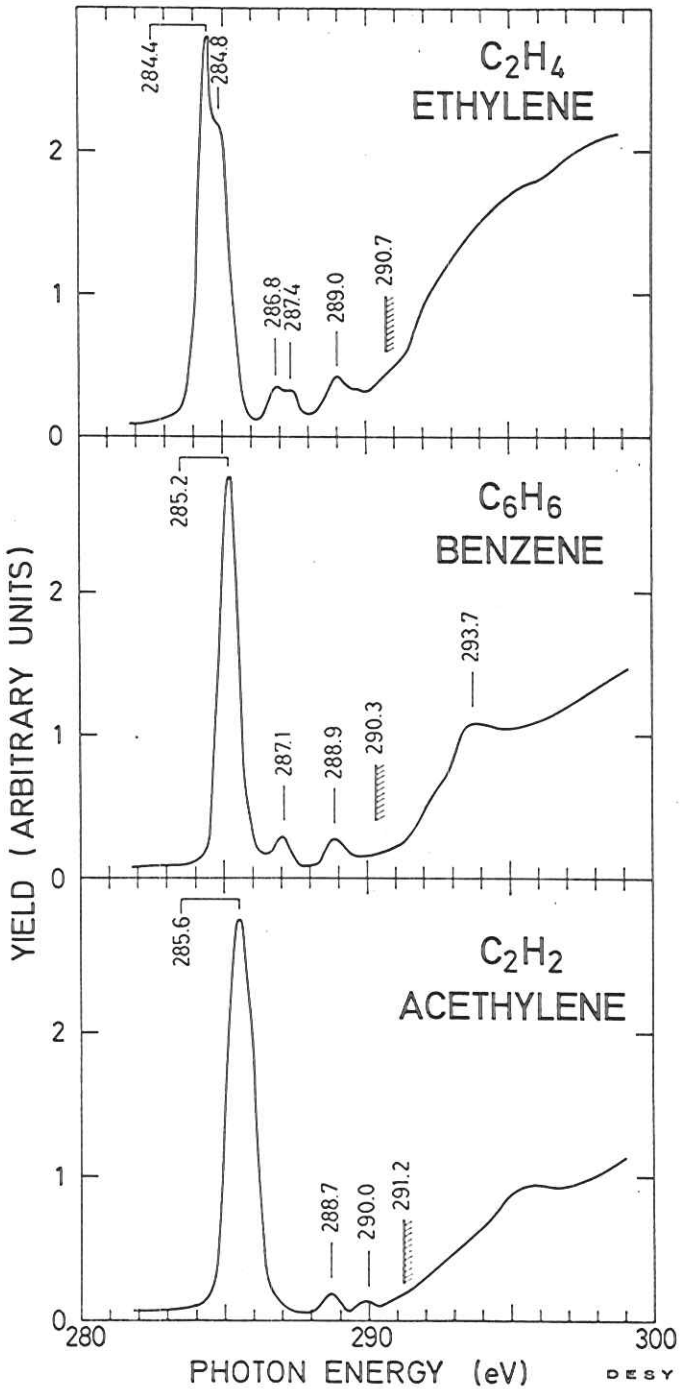
C_2H_4
ETHYLENE
284.4
284.8
286.8
287.4
289.0
290.7
C_6H_6
BENZENE
285.2
287.1
288.9
290.3
293.7
C_2H_2
ACETHYLENE
285.6
288.7
290.0
291.2
YIELD (ARBITRARY UNITS)
PHOTON ENERGY (eV)
280
290
300
DESY
24382

Fig.2o

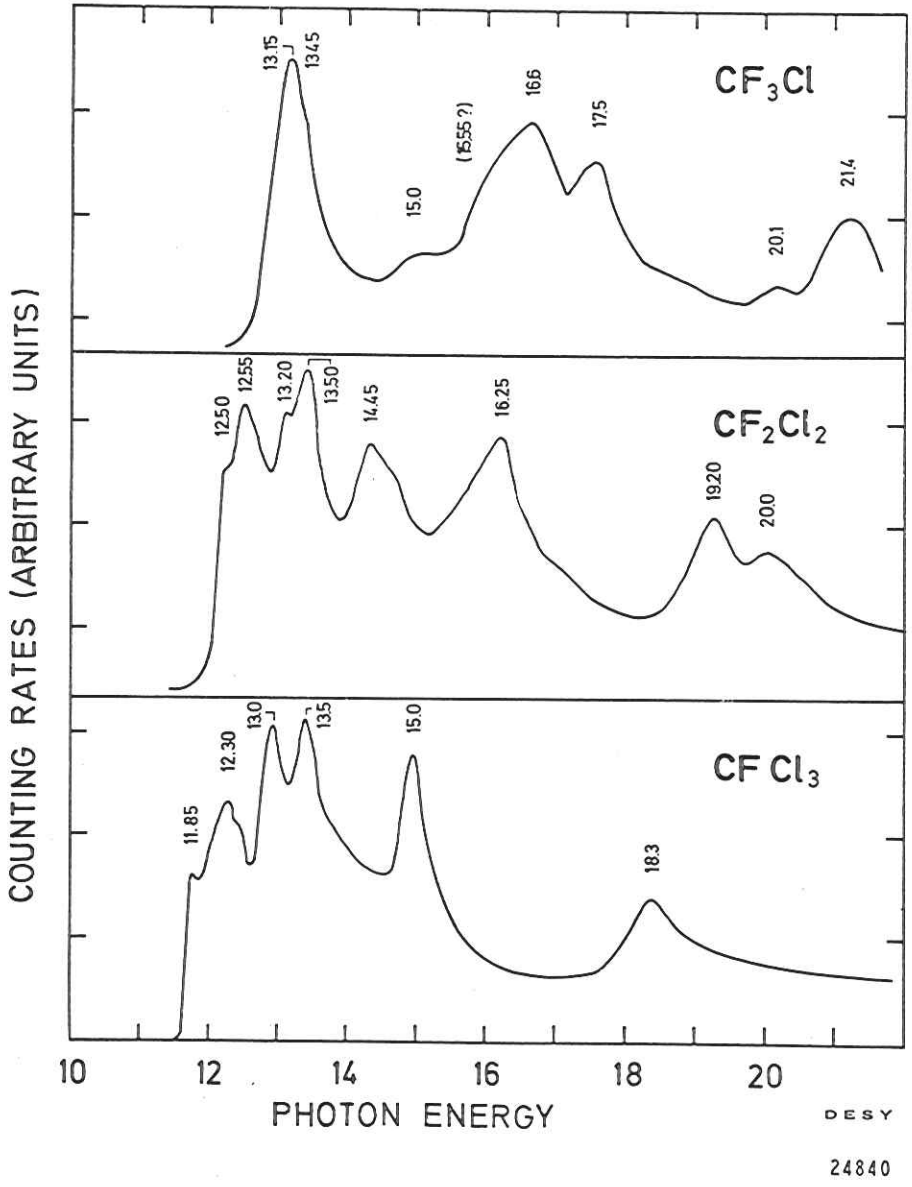
COUNTING RATES (ARBITRARY UNITS)
CF3Cl
13.15
13.45
15.0
(15.55?)
16.6
17.5
20.1
21.4
CF2Cl2
12.50
12.55
13.20
13.50
14.45
16.25
19.20
20.0
CFCl3
11.85
12.30
13.0
13.5
15.0
18.3
10
12
14
16
18
20
PHOTON ENERGY
DESY
24840

Fig.21

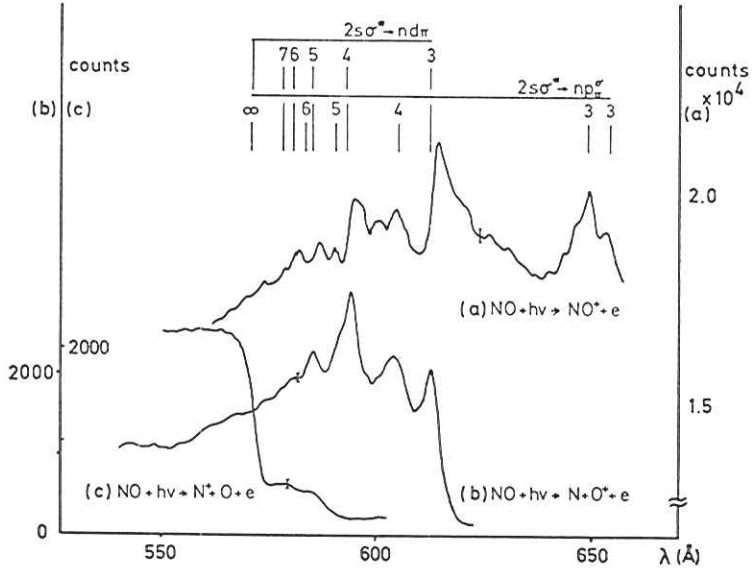
counts
(b) (c)
2sσ*→ndπ
7 6 5 4 3
2sσ*→npπ
∞ 6 5 4 3 3
counts
(a) x10^4
2.0
1.5
2000
2000
0
(a) NO+hv → NO+ + e
(c) NO + hv → N+ + O + e
(b) NO + hv → N + O+ + e
550
600
650
λ (Å)

Fig.22

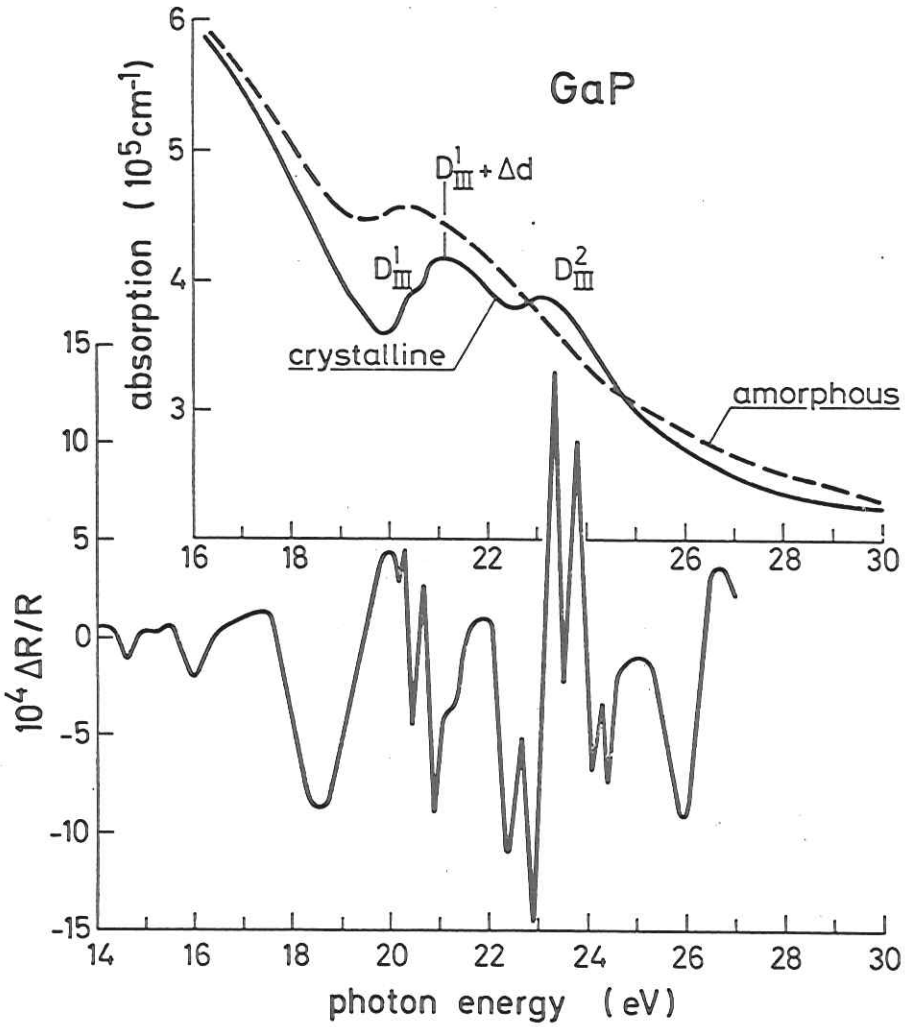
GaP
absorption ($10^5 cm^{-1}$)
$D^1_{III} + \Delta d$
D^1_{III}
D^2_{III}
crystalline
amorphous
$10^4 \Delta R/R$
photon energy (eV)

Fig.23

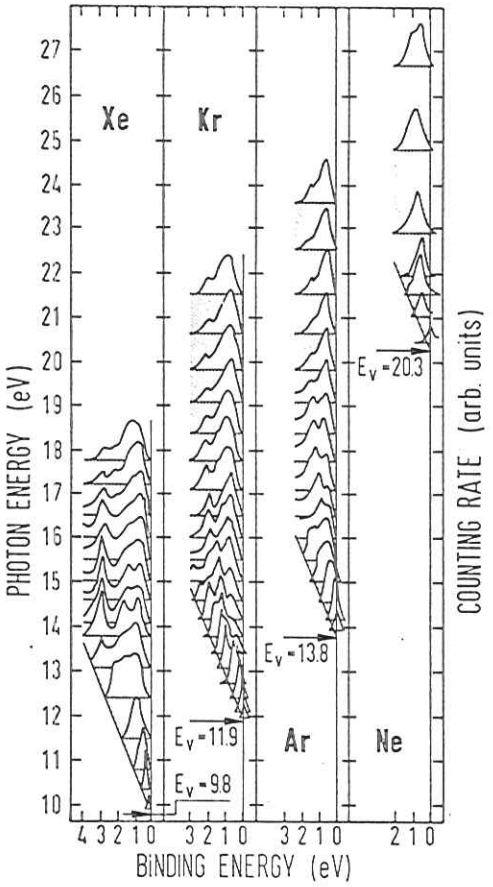
Xe
Kr
Ar
Ne
E_v = 20.3
E_v = 13.8
E_v = 11.9
E_v = 9.8
PHOTON ENERGY (eV)
COUNTING RATE (arb. units)
BINDING ENERGY (eV)

Fig.24

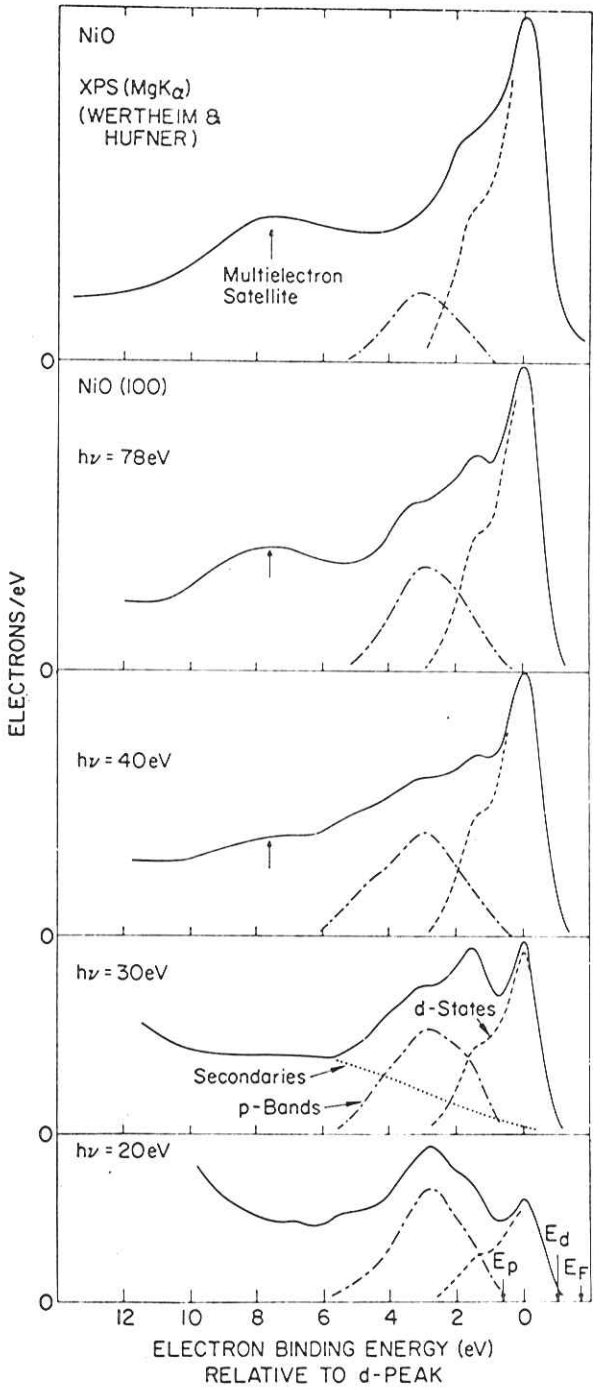
NiO
XPS (MgKα)
(WERTHEIM & HUFNER)
Multielectron Satellite
NiO (100)
hν = 78eV
hν = 40eV
hν = 30eV
d-States
Secondaries
p-Bands
hν = 20eV
E_d
E_p
E_F
ELECTRONS/eV
0
12 10 8 6 4 2 0
ELECTRON BINDING ENERGY (eV)
RELATIVE TO d-PEAK

Fig.25

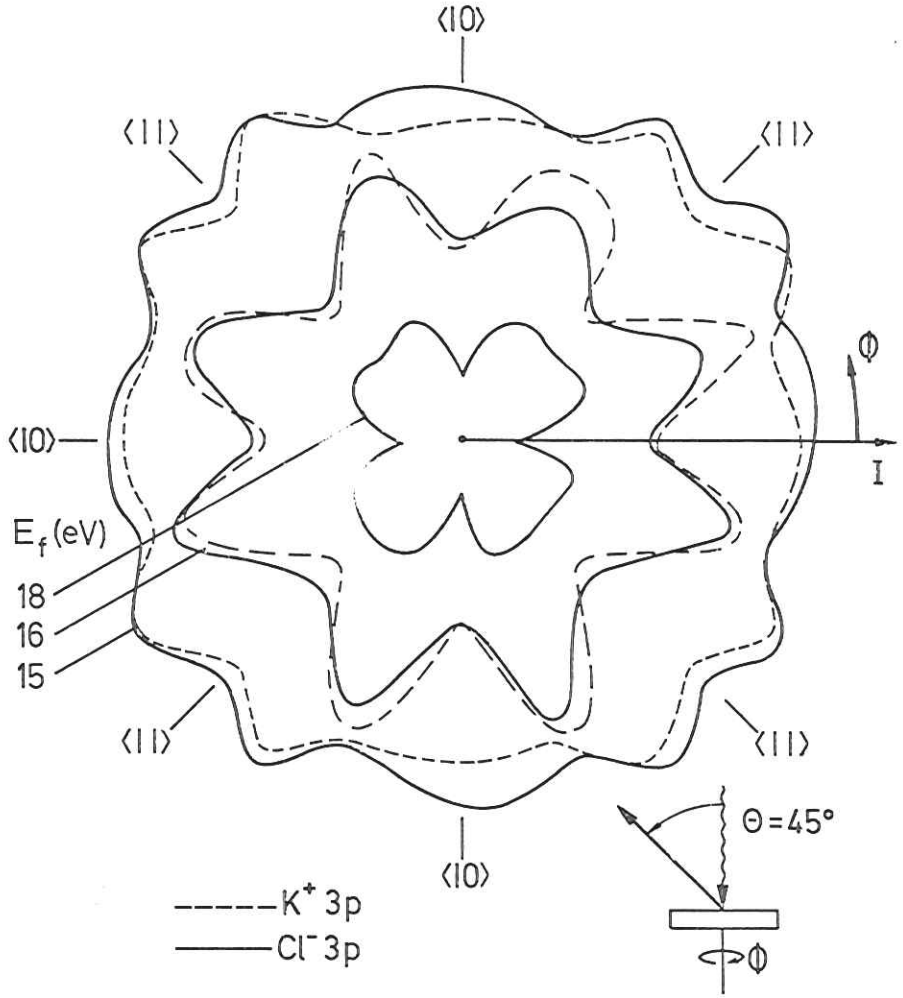
⟨10⟩
⟨11⟩
⟨11⟩
⟨10⟩
Φ
I
E_f (eV)
18
16
15
⟨11⟩
⟨11⟩
⟨10⟩
Θ=45°
-----K⁺ 3p
——Cl⁻ 3p
Φ

Fig.26

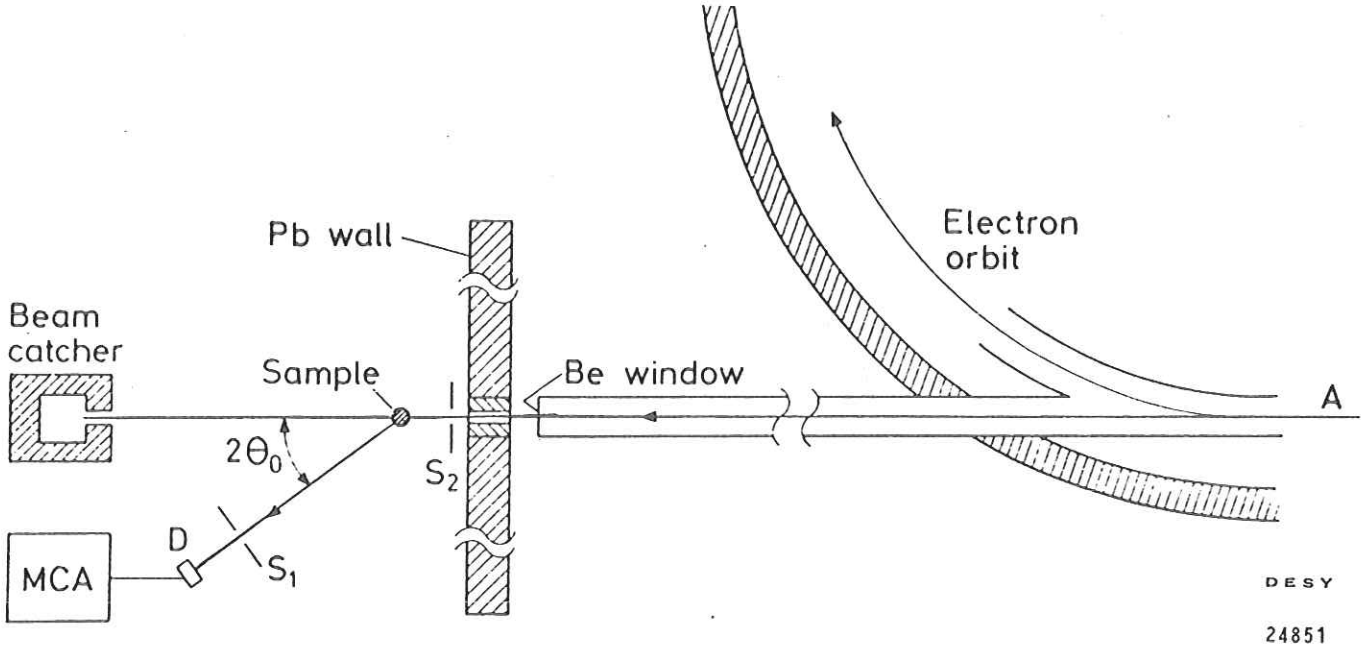
Pb wall
Electron
orbit
Beam
catcher
Sample
Be window
A
$2\Theta_0$
S_2
D
MCA
S_1
DESY
24851

Fig.28

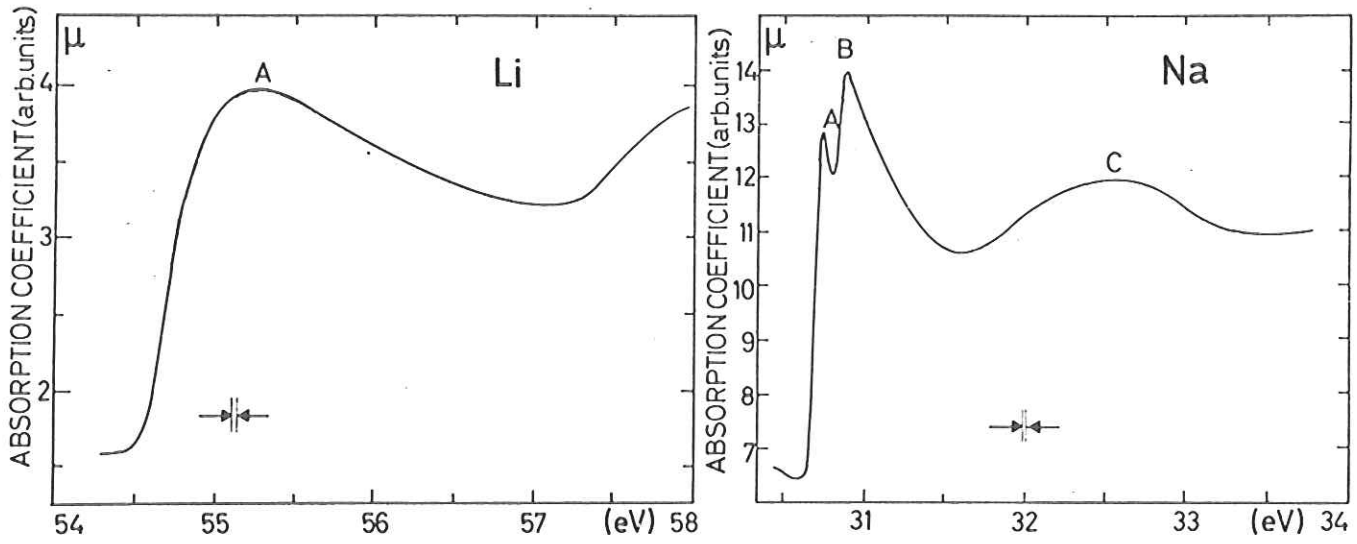
μ
Li
A
ABSORPTION COEFFICIENT (arb.units)
4
3
2
54
55
56
57
(eV) 58
μ
Na
B
A
C
14
13
12
11
10
9
8
7
31
32
33
(eV) 34
DESY
24700

Fig.27

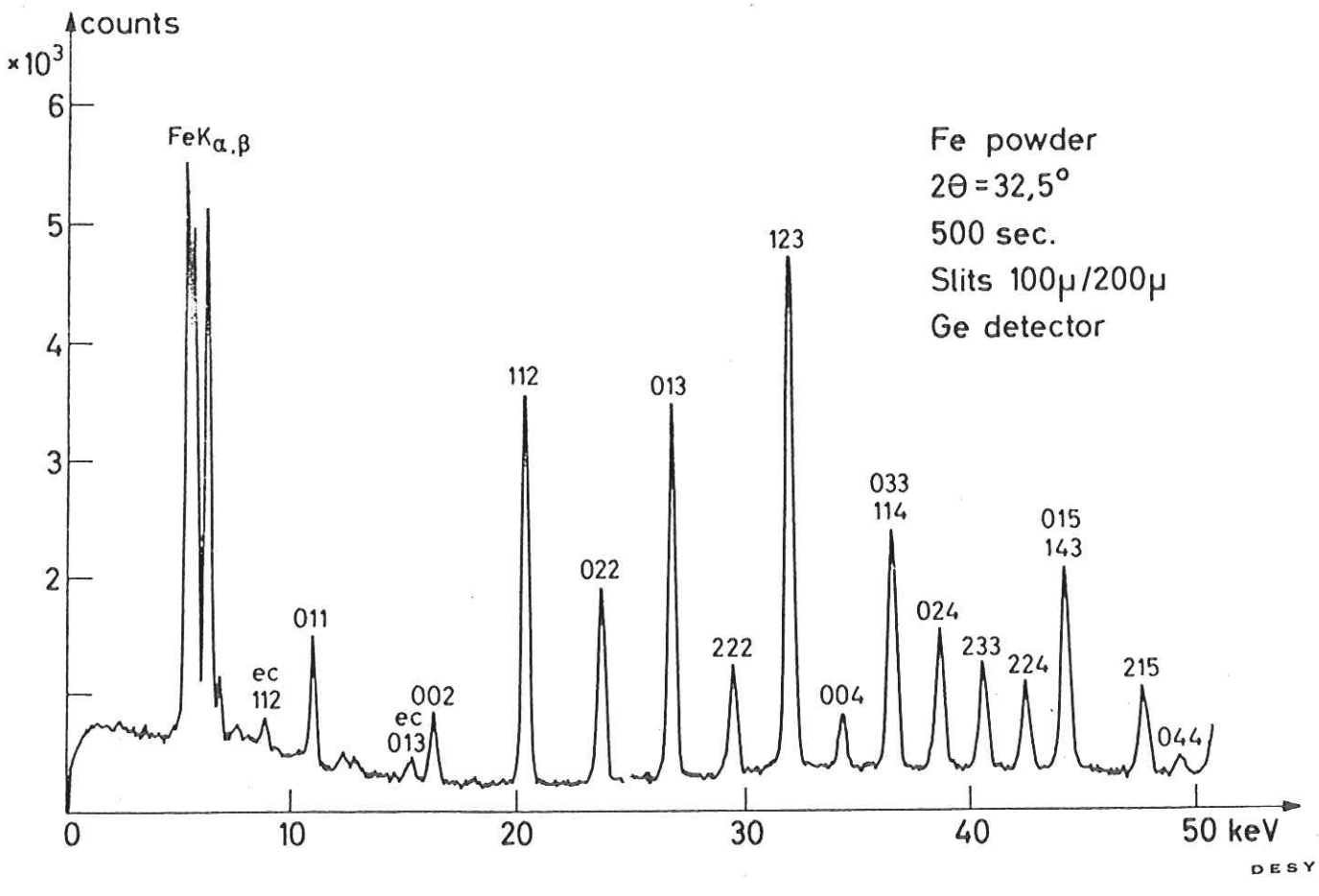
counts
×10³
6
5
4
3
2
FeKα,β
ec
112
011
ec
013
002
112
022
013
222
123
004
033
114
024
233
224
015
143
215
044
Fe powder
2θ = 32,5°
500 sec.
Slits 100μ/200μ
Ge detector
0
10
20
30
40
50 keV
DESY
24848

Fig.29

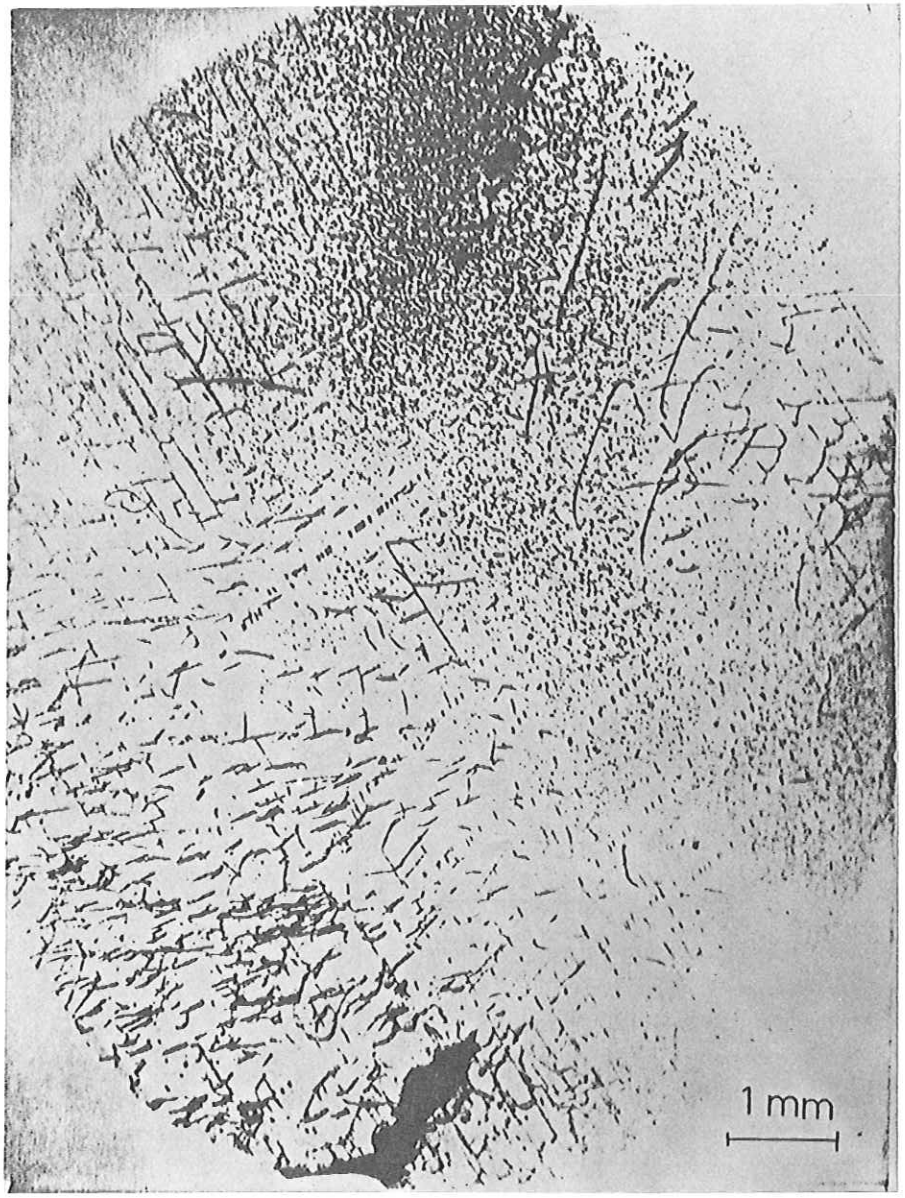

Fig.30

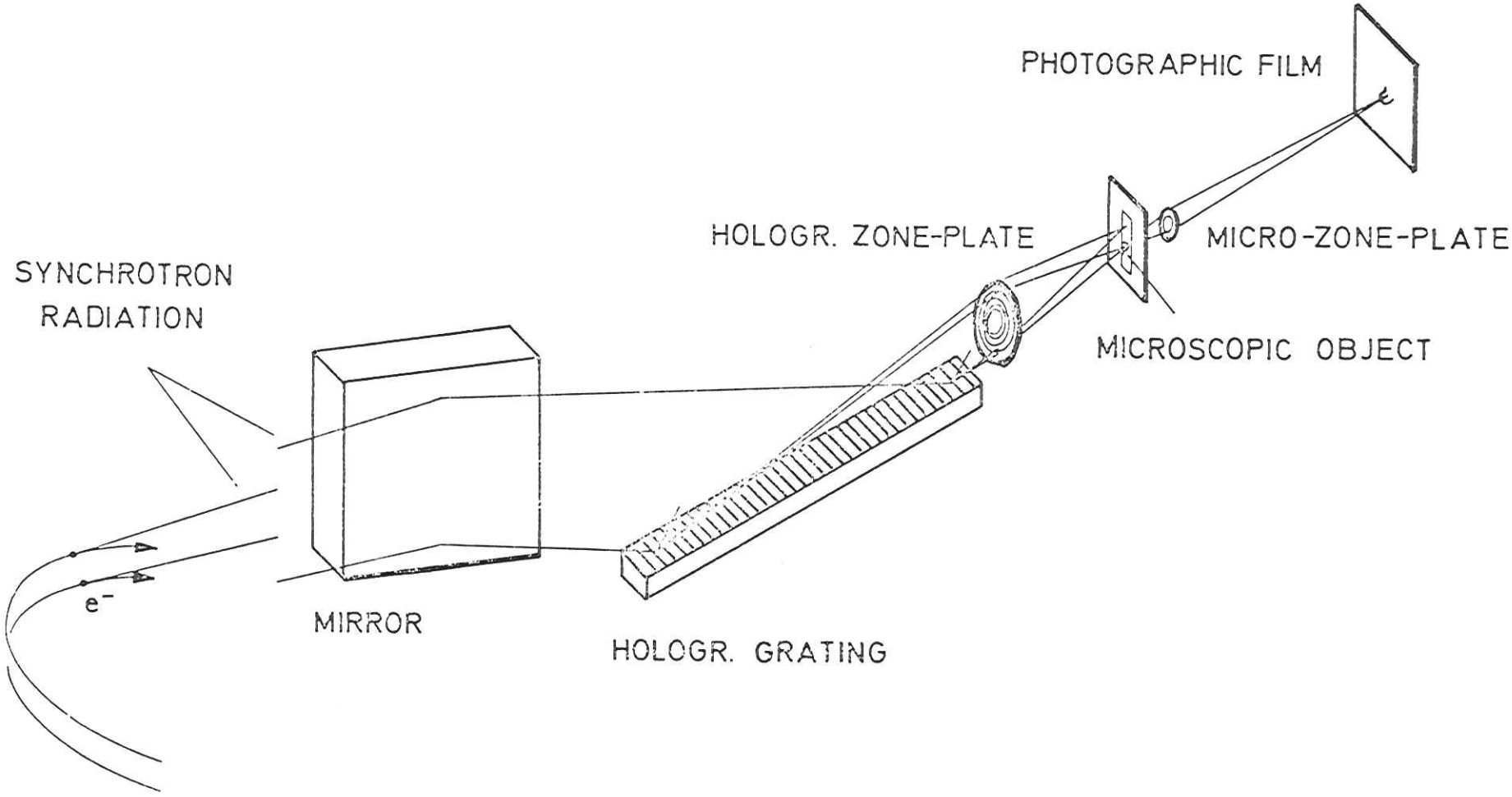

ZONE-PLATE-MICROSCOPE FOR-X RAYS

DESY

24843

Fig. 31

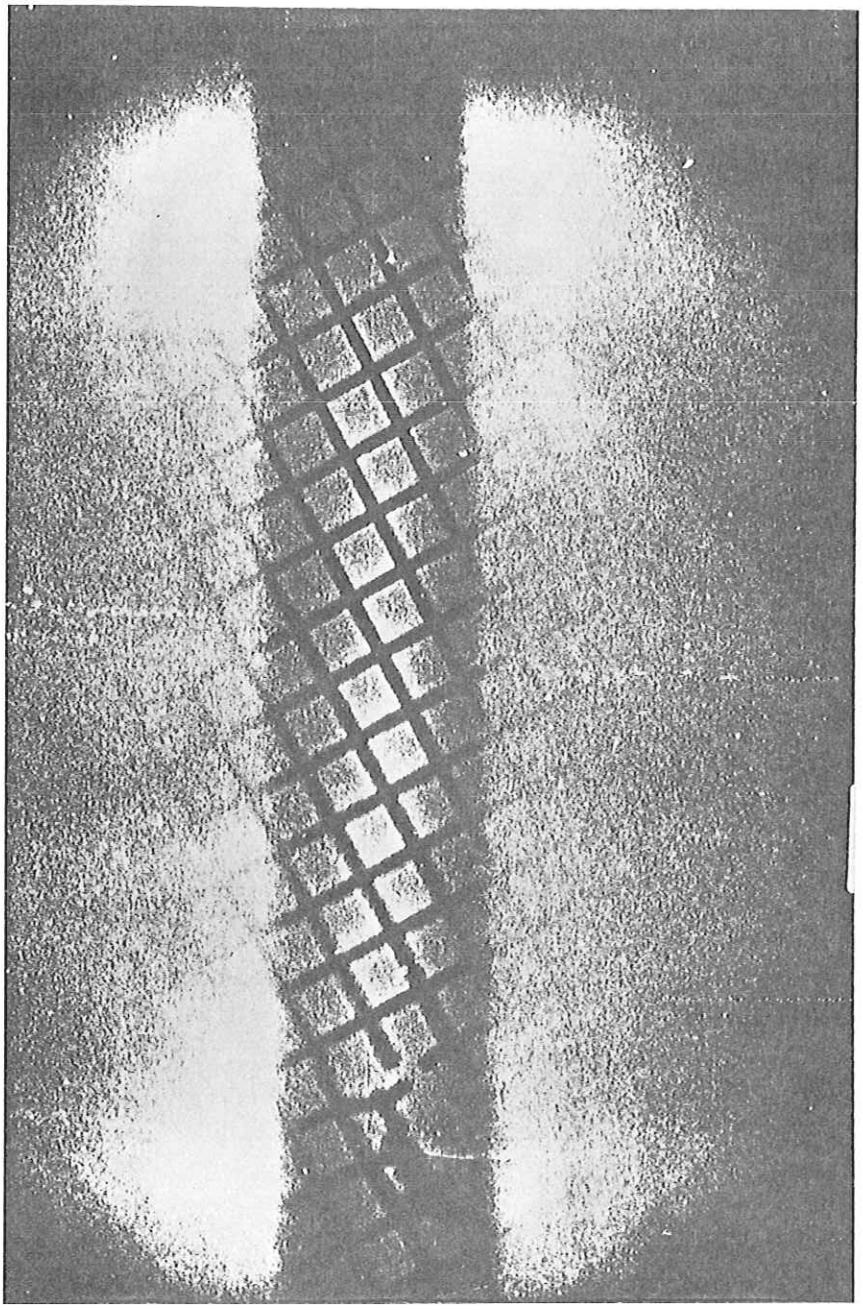

Fig.32

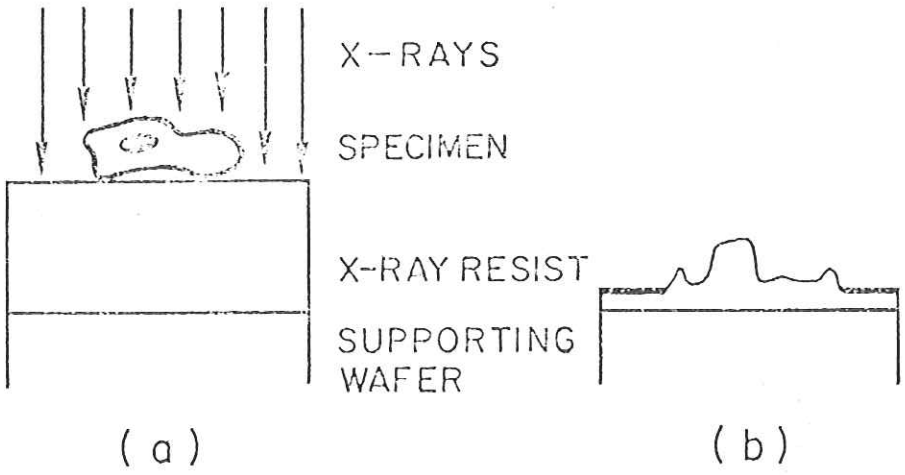

Fig. 33

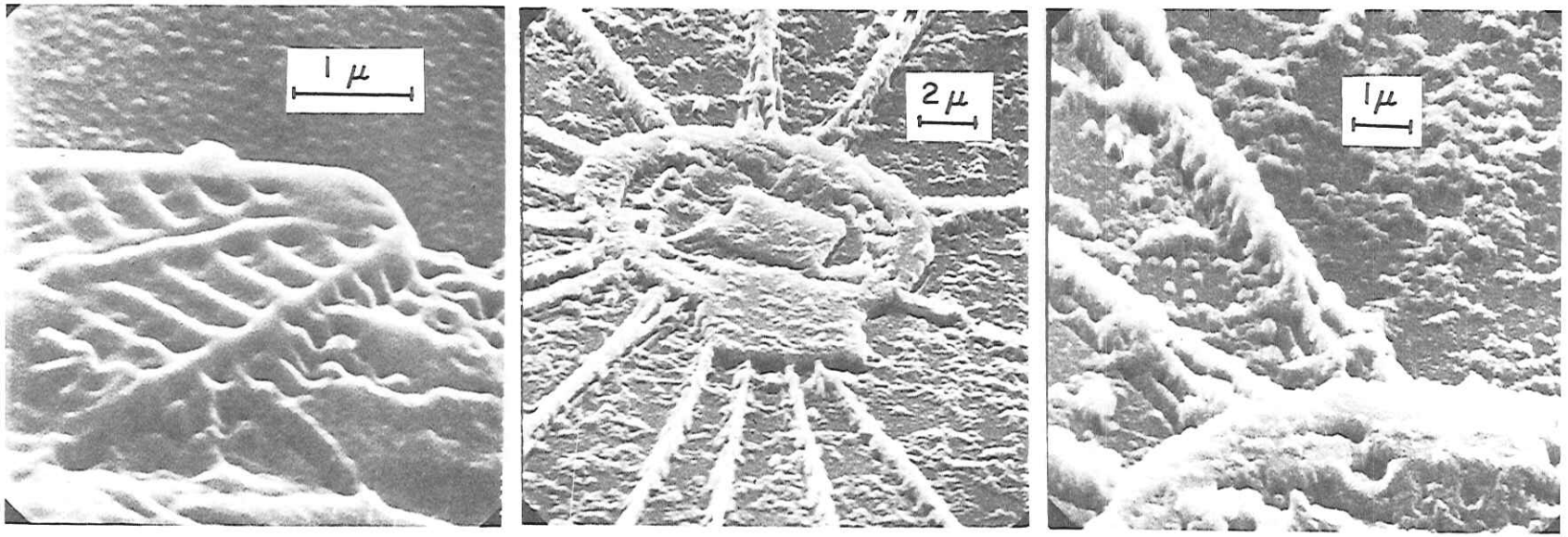

Fig.34